THE JOURNAL OF BIOLOGICAL CHEMISTRY VOL. 290, NO. 32, pp. 19544–19557, August 7, 2015
Published in the U.S.A.

G Protein-coupled Receptor 40 (GPR40) and Peroxisome Proliferator-activated Receptor γ (PPARγ)

*AN INTEGRATED TWO-RECEPTOR SIGNALING PATHWAY**

Received for publication, January 15, 2015, and in revised form, June 10, 2015 Published, JBC Papers in Press, June 23, 2015, DOI 10.1074/jbc.M115.638924

Shuibang Wang[1], Keytam S. Awad, Jason M. Elinoff, Edward J. Dougherty, Gabriela A. Ferreyra, Jennifer Y. Wang, Rongman Cai, Junfeng Sun, Anetta Ptasinska[2], and Robert L. Danner[3]

From the Critical Care Medicine Department, Clinical Center, National Institutes of Health, Bethesda, Maryland 20892

Background: PPARγ ligands are used to treat type 2 diabetes mellitus, but signaling by these drugs is incompletely understood.
Results: Rosiglitazone activation of GPR40 markedly enhanced PPARγ-dependent transcription through downstream effects on p38 MAPK, PGC1α, and EP300.
Conclusion: GPR40 and PPARγ can function as an integrated two-receptor signal transduction pathway.
Significance: Future drug development should consider the effects of prospective ligands at both receptors.

Peroxisome proliferator-activated receptor γ (PPARγ) ligands have been widely used to treat type 2 diabetes mellitus. However, knowledge of PPARγ signaling remains incomplete. In addition to PPARγ, these drugs also activate G protein-coupled receptor 40 (GPR40), a $G\alpha_q$-coupled free fatty acid receptor linked to MAPK networks and glucose homeostasis. Notably, p38 MAPK activation has been implicated in PPARγ signaling. Here, rosiglitazone (RGZ) activation of GPR40 and p38 MAPK was found to boost PPARγ-induced gene transcription in human endothelium. Inhibition or knockdown of p38 MAPK or expression of a dominant negative (DN) p38 MAPK mutant blunted RGZ-induced PPARγ DNA binding and reporter activity in EA.hy926 human endothelial cells. GPR40 inhibition or knockdown, or expression of a DN-$G\alpha_q$ mutant likewise blocked activation of both p38 MAPK and PPARγ reporters. Importantly, RGZ induction of PPARγ target genes in primary human pulmonary artery endothelial cells (PAECs) was suppressed by knockdown of either p38 MAPK or GPR40. GPR40/PPARγ signal transduction was dependent on p38 MAPK activation and induction of PPARγ co-activator-1 (PGC1α). Silencing of p38 MAPK or GPR40 abolished the ability of RGZ to induce phosphorylation and expression of PGC1α in PAECs. Knockdown of PGC1α, its essential activator SIRT1, or its binding partner/co-activator EP300 inhibited RGZ induction of PPARγ-regulated genes in PAECs. RGZ/GPR40/p38 MAPK signaling also led to EP300 phosphorylation, an event that enhances PPARγ target gene transcription. Thus, GPR40 and PPARγ can function as an integrated two-receptor signal transduction pathway, a finding with implications for rational drug development.

Obesity-associated type 2 diabetes mellitus has reached epidemic proportions in the United States and is a major risk factor for coronary artery disease and stroke (1). Thiazolidinediones (TZDs),[4] synthetic insulin-sensitizing drugs that activate peroxisome proliferator-activated receptor γ (PPARγ), have been widely used to treat this disease (2, 3). In addition to lowering glucose levels (3), TZDs also lower blood pressure (4), improve lipid profiles (5), and reduce vascular inflammation (6). These effects in non-adipose tissues have raised the possibility that PPARγ ligands may be more broadly useful in vascular disorders, such as atherosclerosis (7), pulmonary arterial hypertension (8), and septic shock (9). However, side effects, including weight gain, fluid retention, congestive heart failure, and bone fractures, have been linked to TZDs (10). These adverse effects underscore our still incomplete understanding of PPARγ signaling and the need to develop safer, more effective PPARγ ligands (10).

The direct binding of TZDs and other ligands to PPARγ activates two major but distinct signal transduction pathways. *Cis*-activation drives transcription through ligand-dependent recruitment of co-activators, such as PPARγ co-activator-1α (PGC1α), PPARγ dimerization with the retinoid X receptor (11), and the binding of this complex to peroxisome proliferator response elements (PPREs) in the promoter region of target genes. *Trans*-repression of inflammatory response genes re-

* This work was supported, in whole or in part, by National Institutes of Health intramural funds. The authors declare that they have no conflicts of interest with the contents of this article.

[1] To whom correspondence may be addressed: Critical Care Medicine Department, National Institutes of Health, 10 Center Dr., Rm. 2C145, Bethesda, MD 20892-1662. Tel.: 301-496-9320; Fax: 301-402-1213; E-mail: swang@cc.nih.gov.
[2] Present address: Institute of Biomedical Research, College of Medical and Dental Sciences, University of Birmingham, Birmingham B15 2TT, United Kingdom.
[3] To whom correspondence may be addressed: Critical Care Medicine Dept., National Institutes of Health, 10 Center Dr., Rm. 2C145, Bethesda, MD 20892-1662. Tel.: 301-496-9320; Fax: 301-402-1213; E-mail: rdanner@nih.gov.

[4] The abbreviations used are: TZDs, thiazolidinediones; PPARγ, peroxisome proliferator-activated receptor γ; PGC1α, PPARγ co-activator-1α; PPRE, peroxisome proliferator response elements; CBP, CREB-binding protein; CREB, cAMP-response element-binding protein; GPR40, G-protein-coupled receptor 40; RGZ, rosiglitazone; PGZ, pioglitazone; L-NAME, N^{ω}-nitro-L-arginine methyl ester hydrochloride; DTANO, DETA NONOate; SB, SB202190; CAT, chloramphenicol acetyltransferase; LUC, luciferase; DN-p38, dominant negative p38 MAPK; DN-$G\alpha_q$, dominant negative G-protein α_q; PAEC, primary human pulmonary artery endothelial cell; CTRL, control.

quires the covalent modification of PPARγ at lysine 395 by the small ubiquitin-like modifier with subsequent tethering of PPARγ to nuclear receptor co-repressor and histone deacetylase complexes at NFκB and AP-1 sites (12).

Besides these primary ligand-dependent pathways, adjunctive post-translational modifications of PPARγ and its co-activators also regulate PPARγ signaling. ERK and JNK directly phosphorylate PPARγ on serine 112 and inhibit its transcriptional activation (13–16). Cyclin-dependent kinase 5 phosphorylates PPARγ on serine 273, modulating the PPARγ transcriptional program (17). Furthermore, p38 MAPK phosphorylation of PGC1α (18–21) and CBP/EP300 (22) facilitate chromatin remodeling and PPARγ-dependent transcription. PGC1α, a key regulator of PPARγ, is additionally acetylated by GCN5 (23) and deacetylated by SIRT1 (24, 25), reducing and enhancing its co-transcriptional activity, respectively.

Although the anti-diabetic activity of TZDs was first reported in 1982 (26), recognition as ligand/agonists of the orphan nuclear receptor PPARγ came more than a decade later (27, 28). More recently, TZDs were found to bind to and activate $G\alpha_q$ protein-coupled receptor 40 (GPR40) (29–34), a cell membrane receptor associated with free fatty acid- and glucose-induced insulin secretion (35, 36), effects that overlap with those of PPARγ (37, 38). Importantly, GPR40 signaling causes rapid activation of ERK, p38 MAPK, and JNK (31, 33). Whereas we previously found that •NO activation of p38 MAPK initiated PPARγ signaling in human endothelial cells (39), others have also associated p38 MAPK with PPARγ-related effects in adipocytes (20, 40). Collectively, these results suggest that TZD signaling through GPR40 with subsequent activation of p38 MAPK might modulate PPARγ transcriptional activity in human endothelium.

This investigation sought to determine whether TZD activation of GPR40 and p38 MAPK influences PPARγ signaling in human endothelial cells and, if so, to explore the underlying mechanism. A two-receptor paradigm for PPARγ signal transduction is proposed with implications for the development of PPARγ therapeutics.

Experimental Procedures

Reagents—Rosiglitazone (RGZ), pioglitazone (PGZ), N^{ω}-nitro-L-arginine methyl ester hydrochloride (L-NAME), and DETA NONOate (DTANO) were obtained from Cayman Chemical (Ann Arbor, MI). SB202190 (SB) was from EMD Chemicals (Gibbstown, NJ). GW1100 was purchased from OTAVA Ltd. (Ontario, Canada). PPRE reporter constructs containing three copies of PPRE upstream of the reporter gene 3-thymidine kinase-chloramphenicol acetyltransferase (PPRE-CAT) or 3-thymidine kinase-luciferase (PPRE-LUC), were kindly supplied by Dr. Ronald M. Evans (Salk Institute, La Jolla, CA) (41). Dr. Ae-Kyung Yi (University of Tennessee Health Science Center) provided the dominant negative p38 MAPK (DN-p38 MAPK) expression plasmid (42). The dominant-negative G-protein α_q mutant (DN-$G\alpha_q$; Q209L/D277N) expression plasmid was obtained from the UMR cDNA Resource Center (University of Missouri, Rolla. MO). This mutant has a lowered affinity for guanine nucleotides and an enhanced affinity for xanthine nucleotides, resulting in stable and specific complexes with cognate receptors that compete with endogenous wild-type G-proteins (43). Expression plasmids for $PPAR\gamma_2$ (catalogue no. 8895), EP300 (catalogue no. 23252), and PGC1α (catalogue no. 10974) were purchased from Addgene Inc. (Cambridge, MA). The GPR40 expression plasmid was from OriGene (Rockville, MD). FuGENE® 6 transfection reagent, plasmid pRL-TK expressing *Renilla* luciferase, used as an internal control for cell transfection, and the Dual-Luciferase® reporter assay system were from Promega (Madison, WI). Specific On-TARGETplus SMARTpool siRNA for p38α MAPK, GPR40, PGC1α, SIRT1, or EP300 and control siGENOME non-targeting siRNA were purchased from Dharmacon Inc. (Lafayette, CO). Specific GPR40 shRNA pool and its control plasmid were from Qiagen Inc. (Valencia, CA). Specific TaqMan® primers/probes were purchased from Applied Biosystems (Foster City, CA).

Cell Culture—EA.hy926 cells, a hybrid human endothelial cell line, were obtained from ATCC (Manassas, VA). A retrovirus-transfected HeLaS cell line, stably expressing FLAG-tagged PPARγ (HeLaS/F-PPARγ), was kindly provided by Dr. Kai Ge (National Institutes of Health, NIDDK, Bethesda, MD) (44). Both EA.hy926 and HeLaS/F-PPARγ cell lines were maintained in DMEM supplemented with 10% FBS, D-glucose (4.5 g/liter), L-glutamine (2 mmol/liter), sodium pyruvate (1 mmol/liter), penicillin (100 units/ml), and streptomycin (100 mg/ml). Primary human pulmonary artery endothelial cells (PAECs) were purchased from Lonza (Walkersville, MD) and used at passages 1–4. PAECs were cultured in endothelial growth medium 2 (EGM2™) supplemented with growth factors (EGM2™ SingleQuot kit) from Lonza containing 2% FBS on flasks precoated with type I collagen (BD Biosciences). In experiments using TZDs, charcoal-stripped FBS was used instead of regular FBS. Phenol red-free DMEM was used in experiments using DTANO or L-NAME.

Reporter Gene Assay—EA.hy926 cells (2×10^5/2 ml/well) were seeded in 6-well plates 16 h prior to transfection with 100 ng of PPRE reporter (PPRE-CAT or PPRE-LUC), 100 ng of internal control pRL-TK, and 50 ng of $PPAR\gamma_2$ expression plasmid in the presence or absence of additional expression plasmids, including DN-p38 MAPK, DN-$G\alpha_q$, GPR40, PGC1α, and EP300, as indicated. FuGENE® 6 transfection reagent was utilized at a ratio of 3 μl/μg of DNA. Twenty-four hours after transfection, cells were treated for an additional 24 h as indicated in the corresponding figure legends. Chloramphenicol acetyltransferase and luciferase activities were then measured using the CAT ELISA (Roche Diagnostics) and the Dual-Luciferase® reporter assay system (Promega), respectively. In reporter experiments with gene knockdown, cells were co-transfected with siRNA, shRNA, or their controls for 48 h, followed by 24-h stimulation. Non-targeting control or p38α MAPK siRNA was transfected using Nucleofector kits (Amaxa, Gaithersburg, MD), as described previously (39). GPR40 shRNA pool or its control plasmid was transfected using FuGENE® 6.

PAEC siRNA Silencing—PAECs (2×10^5/2 ml/well) were seeded in 6-well plates 16 h prior to transfection. GPR40, p38α MAPK, PGC1α, SIRT1, and EP300 siRNAs or non-targeting siRNA controls (30 nM) were transfected using DharmaFECT 1 (Dharmacon Inc.) in OPTI-MEM medium (Life Technologies,

Inc.). Eight hours post-transfection, cells were washed once with PBS and cultured for 48 h in EGM2™ medium supplemented with growth factors and charcoal-stripped fetal calf serum, followed by treatment with RGZ for 24 h before measurement of PPARγ target gene mRNA or protein.

Detection of PPARγ Binding to Specific DNA Sequence—EA.hy926 cells were treated for 1 h with RGZ (10 μM) or vehicle control with or without SB (1 μM) pretreatment for 40 min, as indicated. Nuclear extracts (3–4 μg) were then prepared for TransAM® PPARγ ELISA (Active Motif, Carlsbad, CA), which detects human PPARγ$_{1/2}$ binding to PPRE consensus sequence and does not cross-react with PPARα or PPARβ.

Western Blotting and Quantitative Real-time TaqMan® PCR—For Western blotting, samples (30 μg of whole cell lysates) were applied to a 4–12% Novex® Tris-glycine gel (Invitrogen) or a 4–15% Mini-PROTEAN® TGX gel (Bio-Rad) and subjected to electrophoretic separation. Separated protein was electrically transferred to a nitrocellulose membrane. The blot was blocked with 5% nonfat dry milk in PBS with 1% Tween® 20. Anti-phospho-p38 MAPK (pp38, catalog no. 4631), anti-total p38 MAPK (p38, catalog no. 9212), anti-PPARγ (catalog no. 2430), anti-EP300 (catalog no. D9B6; all from Cell Signaling Technology Inc., Danvers, MA), anti-GPR40 (catalog no. 3393-1; Epitomics, Burlingame, CA), and anti-SIRT1 (catalog no. 07-131; Millipore, Billerica, MA) primary antibodies were all used at a 1:1000 dilution. Anti-PGC1α (catalog no. 101707; Cayman Chemical) and anti-phospho-EP300 primary antibodies (anti-Ser(P)-1834; catalog no. PA5-12735; Thermo Scientific, Rockford, IL) were used at 1:200 and 1:500 dilutions, respectively. A secondary antibody, horseradish peroxidase-conjugated goat anti-rabbit IgG, was used at a 1:10,000 dilution. All antibodies were diluted in 5% nonfat dry milk in PBS with 1% Tween® 20. The protein bands were detected using SuperSignal® West Femto chemiluminescence substrate (Thermo Scientific). Densitometry analysis of blots was performed using Image Lab™ software (Bio-Rad).

Total RNA was extracted using the RNeasy kit (Qiagen), and cDNA was synthesized with iScript™ cDNA synthesis kits (Bio-Rad). TaqMan® PCR was performed with the Applied Biosystems Vii™ 7 instrument.

Immunoprecipitation—PAECs were transfected with various siRNAs, as indicated. Forty-eight hours post-transfection, cells were treated with RGZ (10 μM) or vehicle control for 1 and 4 h to examine effects on PGC1α phoshorylation and acetylation, respectively, before preparation of nuclear protein and whole cell lysates. Immunoprecipitation of nuclear protein (40 μg) was performed with anti-phosphoserine (catalog no. AB1603) and anti-phosphothreonine (catalog no. AB1607) antibodies from Millipore. Immunoprecipitation of whole cell lysates (500 μg) used anti-acetyl-lysine antibody (catalog no. 06-933; Millipore). After incubation with rotation at 4 °C overnight, Dynabeads® protein G (1.5 mg; Invitrogen) was added. Immunoprecipitates were then subjected to Western blotting with anti-PGC1α antibody (catalog no. 101707; Cayman Chemical).

Chromatin Immunoprecipitation (ChIP) Assay—PAECs were pretreated with SB (10 μM), GW1100 (20 μM), or vehicle control (CTRL) for 40 min and then incubated with RGZ (10 μM) or vehicle CTRL for another 24 h. The ChIP assay was carried out using the EZ ChIP™ kit (Millipore) as instructed by the manufacturer. Briefly, cells were cross-linked with 1% formaldehyde and then fragmented using a Misonix sonicator with microtip probe 4418 at a power setting of 4 and a 30% duty cycle. Sonication was performed three times for 10 s with a 50-s cooling on ice between pulses, shearing chromatin into 200–1000-bp fragments. Precipitation was carried out overnight at 4 °C with anti-PPARγ (catalog no. SC-7196; Santa Cruz Biotechnology, Inc., Dallas, TX), anti-EP300 (catalog no. PA1-848; Thermo Scientific), anti-PGC1α (catalog no. ab54481; Abcam Inc., Cambridge, MA), or control mouse IgG. Precipitated protein-DNA complexes were eluted, and cross-linkings were reversed for purification of DNA. PCR was performed using the primers 5′-TTTACTATTTCCACCAGCGGTCTC-3′ and 5′-TCCCCCACACAGCACATTACTG-3′ specific for the −355/−136 region of the human *CD36* promoter that contains three potential PPREs. The PCR products were analyzed by electrophoresis on 2% agarose gels (E-Gel®, Invitrogen), stained with ethidium bromide, and quantified by densitometry.

Statistical Analysis—Data are presented as means ± S.E. For real-time PCR results, geometric means ± S.E. are plotted. All statistical analyses were carried out on log-transformed or Δ cycle threshold data (for real-time PCR) using JMP® version 11 (SAS® Institute Inc., Cary, NC). To analyze continuous dose and time effects, one-way analysis of variance models were used. To test the effects of nominal factors and their interactions, linear mixed models were used, which consider the correlation within each experiment. Non-significant factors were dropped from statistical models to calculate final p values. Post hoc contrasts were tested for our interested comparisons. All p values are two-sided and considered significant if p was <0.05.

Results

Ligand Activation of PPARγ Signaling in EA.hy926 Human Endothelial Cells Is p38 MAPK-dependent—Both RGZ and PGZ (10 μM for each), two clinically relevant TZD PPARγ ligands, activated p38 MAPK in EA.hy926 human endothelial cells ($p \leq 0.002$ for both; Fig. 1, *A* and *B*, respectively). Phosphorylation of p38 MAPK occurred as early as 5 min with a maximal effect at 15 min. As expected, SB (1 μM), a specific p38 MAPK inhibitor, blocked RGZ-induced p38 MAPK phosphorylation ($p < 0.001$ for RGZ *versus* SB plus RGZ; $p = 0.001$ for an interaction between RGZ and SB; Fig. 1*C*). Therapeutic RGZ dosing in humans produces peak plasma concentrations of 1–2 μM (45). In kidney (HEK293T) cells, half-maximal stimulation of PPARγ-dependent transcription was calculated to occur at a RGZ concentration of 6.5 μM (46). Consistent with these results, dose-response testing in HeLaS/F-PPARγ cells found that 10 μM RGZ induced nearly maximal PPRE reporter activity (data not shown). Therefore, subsequent experiments were conducted with RGZ (10 μM) as a prototype for this class of PPARγ ligands. Endogenous PPARγ expression in EA.hy926 endothelial cells is relatively low; therefore, in all experiments directly assessing genomic PPARγ signaling, these cells were transfected with a PPARγ$_2$ expression plasmid (Fig. 1*D*, *inset*). SB (1 μM), a specific p38 MAPK inhibitor that blocked RGZ-induced p38 MAPK phosphorylation (Fig. 1*C*), significantly

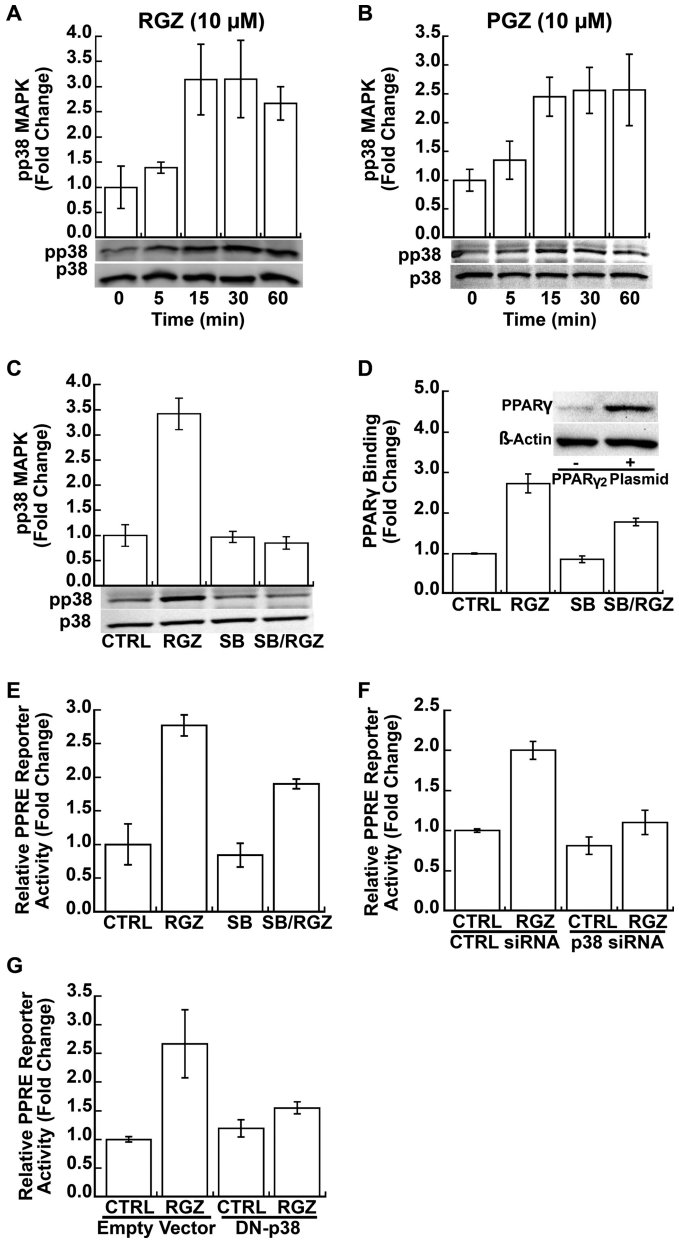

FIGURE 1. **PPARγ ligands induce PPRE-driven transcription through p38 MAPK.** *A* and *B*, RGZ and pioglitazone increased p38 MAPK phosphorylation in EA.hy926 cells ($p < 0.001$ for RGZ effect in *A*; $p = 0.002$ for PGZ effect in *B*). *C*, RGZ-induced p38 MAPK phosphorylation was blocked by SB, a specific p38 MAPK inhibitor ($p < 0.001$ for RGZ *versus* SB plus RGZ; $p = 0.001$ for an interaction between RGZ and SB). Phosphorylated p38 MAPK (*pp38*) and total p38 MAPK (*p38*) were measured by Western blotting. Cells were treated with SB (1 μM) for 40 min and then incubated with RGZ (10 μM) or vehicle CTRL for another 30 min in *C*. Densitometric results for *A–C* of three independent experiments and representative blots are shown. *D*, SB blocked RGZ-induced PPARγ DNA binding, as measured by the TranAM® ELISA ($p = 0.009$ for RGZ *versus* SB plus RGZ). EA.hy926 cells were first transfected with $PPAR\gamma_2$ expression plasmid (*inset*). At 48 h after transfection, cells were treated with SB (1 μM) for 40 min and then incubated with RGZ (10 μM) or vehicle CTRL for another 1 h. *E*, SB (1 μM added 40 min before RGZ or its control) reduced RGZ activation of a PPARγ reporter gene ($p = 0.04$ for RGZ *versus* SB plus RGZ). *F* and *G*, siRNA knockdown of p38α MAPK ($p < 0.001$ for RGZ *versus* p38 siRNA plus RGZ; $p = 0.03$ for an interaction between RGZ and p38 siRNA) or expression of a dominant negative p38 MAPK mutant (DN-p38 MAPK; $p = 0.03$ for RGZ *versus* DN-p38 plus RGZ; $p = 0.04$ for an interaction between RGZ and DN-p38) markedly suppressed RGZ activation of a PPARγ reporter gene. EA.hy926 cells were co-transfected with PPRE-CAT reporter and $PPAR\gamma_2$ expression plasmid with or without p38α MAPK siRNA (p38 siRNA), scrambled CTRL siRNA, a DN-p38 MAPK plasmid, or a control empty vector, as indicated. At 48 h after transfection, cells were treated with RGZ (10 μM) or CTRL for 24 h prior to the measurement of chloramphenicol acetyltransferase activity. Results are presented as means ± S.E. (*error bars*) of three independent experiments in *E–G*.

blocked RGZ-induced PPARγ DNA binding ($p = 0.009$ for RGZ *versus* SB plus RGZ; Fig. 1*D*) and PPRE reporter gene activity ($p = 0.04$ for RGZ *versus* SB plus RGZ; Fig. 1*E*) in EA.hy926 cells. Furthermore, both p38α MAPK siRNA silencing ($p < 0.001$ for RGZ *versus* p38α siRNA plus RGZ; $p = 0.03$ for an interaction between RGZ and p38 siRNA; Fig. 1*F*) and overexpression of a DN-p38 MAPK mutant ($p = 0.03$ for RGZ *versus* DN-p38 plus RGZ; $p = 0.04$ for an interaction between RGZ and DN-p38; Fig. 1*G*) significantly repressed RGZ-induced PPRE reporter activity. The p38α MAPK siRNA used here was previously shown to effectively knockdown p38 MAPK protein in EA.hy926 cells (39).

GPR40 Mediates RGZ Activation of p38 MAPK in EA.hy926 Human Endothelial Cells—Like RGZ, other PPARγ ligands, such as pioglitazone, ciglitazone, and troglitazone, have been shown to bind to $G\alpha_q$-coupled GPR40 (30–32), resulting in rapid activation of p38 MAPK as well as other downstream signaling pathways (31, 33). Notably, GPR40, also known as free fatty acid receptor 1, has been implicated in fatty acid- and glucose-induced insulin secretion (35, 36), effects also regulated by PPARγ (37, 38). EA.hy926 endothelial cells expressed both GPR40 and PPARγ (Fig. 2A), but as noted above, endogenous PPARγ protein expression is relatively low. We next determined whether RGZ activates p38 MAPK via GPR40 in EA.hy926 cells.

GW1100, a specific GPR40 antagonist, inhibited RGZ-induced p38 MAPK phosphorylation ($p < 0.001$ for RGZ *versus* GW1100 plus RGZ; $p = 0.04$ for an interaction between GW1100 and RGZ; Fig. 2*B*). Likewise, shRNA-mediated GPR40 silencing significantly blocked RGZ-induced p38 phosphorylation ($p = 0.006$ for RGZ *versus* GPR40 shRNA plus RGZ; $p = 0.004$ for an interaction between GPR40 shRNA and RGZ; Fig. 2*C*); shRNA knockdown decreased GPR40 protein expression about 50% in EA.hy926 cells ($p = 0.007$ for the main effect of GPR40 shRNA; Fig. 2*D*). These results demonstrate that GPR40 is necessary for RGZ activation of p38 MAPK in a human endothelial line.

Previously, we found that •NO activated p38 MAPK in EA.hy926 cells (39). Therefore, we next examined whether RGZ/GPR40/p38 MAPK signaling might be mediated through •NO as a second messenger. L-NAME, a •NO synthase inhibitor, had no effect on RGZ-induced p38 MAPK phosphorylation ($p = 0.57$ for the main effect of L-NAME; Fig. 2*E*). Conversely, •NO activation of p38 MAPK, which is probably related to its free radical biology (47), was not dependent on GPR40 in EA.hy926 cells. DTANO, a •NO donor, time-dependently induced p38 MAPK phosphorylation ($p = 0.008$; Fig. 2*F*); this phosphorylation was not altered by either GW1100, a specific GPR40 antagonist ($p = 0.55$ for DTANO *versus* GW1100 plus DTANO; Fig. 2*G*) or GPR40 knockdown ($p = 0.61$ for DTANO *versus* GPR40 shRNA plus DTANO; Fig. 2*H*).

RGZ Activation of GPR40 Enhances PPARγ/PPRE-driven Transcription in EA.hy926 Human Endothelial Cells—The above experiments in EA.hy926 human endothelial cells show

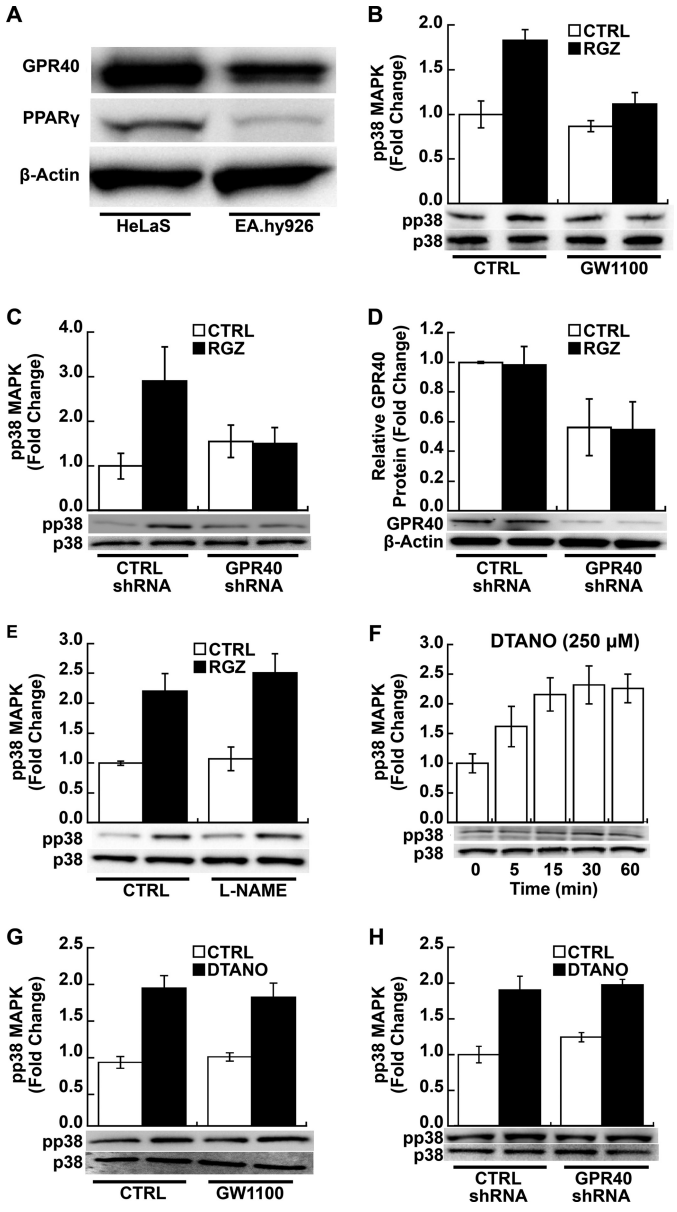

FIGURE 2. **RGZ induces p38 MAPK phosphorylation through GPR40.** *A*, EA.hy926 cells express GPR40 and PPARγ protein as measured by Western blotting; GPR40 and PPARγ expression is shown in a retrovirus-transfected HeLaS cell line, stably expressing PPARγ, as a positive control. A representative blot from four independent experiments is shown. *B*, GW1100, a GPR40 antagonist, blocked RGZ-induced p38 MAPK phosphorylation (pp38) as measured by Western blotting ($p < 0.001$ for RGZ *versus* GW1100 plus RGZ; $p = 0.04$ for an interaction between RGZ and GW1100). EA.hy926 cells were treated with GW1100 (20 μM) or vehicle CTRL for 40 min and then incubated with RGZ (10 μM) or CTRL for another 30 min. *C*, shRNA knockdown of GPR40 blocked RGZ-induced p38 MAPK phosphorylation (*pp38*; $p = 0.006$ for RGZ *versus* GPR40 shRNA plus RGZ; $p = 0.004$ for an interaction between RGZ and GPR40 shRNA). *D*, shRNA knockdown decreased GPR40 protein expression as measured by Western blotting ($p = 0.007$ for the main effect of GPR40 shRNA). EA.hy926 cells were transfected with specific GPR40 shRNA or CTRL shRNA. At 48 h after transfection, cells were treated with RGZ (10 μM) or CTRL for 30 min prior to Western blotting. *E*, L-NAME, a nitric-oxide synthase inhibitor, had no effect on RGZ-induced p38 MAPK phosphorylation (*pp38*) as measured by Western blotting ($p = 0.57$ for the main effect of L-NAME). EA.hy926 cells were treated with L-NAME (1 mM) or vehicle CTRL for 1 h and then incubated with RGZ (10 μM) or CTRL for another 30 min. *F*, DTANO (250 μM), a nitric oxide donor, time-dependently induced p38 MAPK phosphorylation in EA.hy926 cells ($p = 0.008$ for DTANO effect). *G*, GW1100 (20 μM), a specific GPR40 antagonist, did not affect DTANO-induced p38 MAPK phosphorylation in EA.hy926 cells ($p = 0.55$ for DTANO *versus* GW1100 plus DTANO). Cells were treated with GW1100 for 40 min and then incubated with DTANO (250 μM) or CTRL (degraded DTANO) for another 30 min. *H*, GPR40 shRNA did not affect DTANO-induced p38 MAPK phosphorylation, as measured by Western blotting ($p = 0.61$ for DTANO *versus* GPR40 shRNA plus DTANO). EA.hy926 cells were transfected as in *C*. At 48 h after transfection, cells were treated with DTANO (250 μM) or CTRL for 30 min. Densitometric results of independent experiments and a representative blot are shown in *B* ($n = 4$), *C* ($n = 5$), *D* and *E* ($n = 3$), *F* and *G* ($n = 4$), and *H* ($n = 3$). *Error bars*, S.E.

that 1) PPARγ ligands activate p38 MAPK, 2) p38 MAPK modulates PPARγ transcriptional activity, and 3) PPARγ ligand activation of p38 MAPK occurs via GPR40 and is independent of •NO. Next, we tested more directly whether GPR40 signaling modulates ligand-activated PPARγ genomic signaling. Like p38 MAPK silencing and dominant negative mutant (Fig. 1, *F* and *G*), GW1100, a specific GPR40 antagonist, significantly repressed RGZ-induced PPRE reporter activity in EA.hy926 cells ($p < 0.001$ for RGZ *versus* GW1100 plus RGZ; $p = 0.03$ for an interaction between GW1100 and RGZ; Fig. 3*A*). In contrast, GPR40 knockdown reduced both basal and RGZ-stimulated PPRE reporter activity ($p < 0.001$ for GPR40 shRNA main effect; $p = 0.32$ for an interaction between RGZ and GPR40 shRNA; Fig. 3*B*). Overexpression of DN-$G\alpha_q$, a mutant that competes with endogenous wild-type G-proteins for GPR40 coupling (43), also blocked both basal and RGZ-induced PPRE reporter activity ($p < 0.001$ for DN-$G\alpha_q$ mutant main effect; $p = 0.88$ for an interaction between RGZ and DN-$G\alpha_q$; Fig. 3*C*). In addition, GPR40 overexpression enhanced both basal and RGZ-induced PPARγ transcriptional activity ($p < 0.001$ for GPR40 plasmid main effect; $p = 0.11$ for an interaction between RGZ and GPR40 plasmid; Fig. 3*D*). Consistent with our findings for RGZ-induced p38 MAPK activation (Fig. 2*E*), L-NAME (0–1 mM), a •NO synthase inhibitor, did not affect basal or RGZ-induced PPRE reporter activity ($p = 0.25$ for the main effect of L-NAME; Fig. 3*E*), further evidence that •NO plays no role in RGZ/GPR40/p38 MAPK/PPARγ signaling in EA.hy926 cells.

RGZ/GPR40/p38 MAPK Signaling Boosts the Transcription of PPARγ Target Genes in PAECs—The RGZ/GPR40/p38 MAPK/PPARγ signaling transduction pathway was further explored in PAECs. Similar to EA.hy926 cells, a hybrid human endothelial line, RGZ increased p38 MAPK phosphorylation ~2-fold in PAECs ($p < 0.001$ for RGZ *versus* control within the control siRNA condition; Fig. 4*A*), and siRNA silencing of p38α blocked this effect ($p = 0.43$ for RGZ *versus* control within the p38 MAPK siRNA condition; $p = 0.009$ for an interaction between p38 MAPK siRNA and RGZ; Fig. 4*A*). Knockdown of p38α MAPK decreased total p38 MAPK protein about 80% ($p < 0.001$ for the main effect of p38α MAPK siRNA; Fig. 4*A*). PAECs expressed PPARγ protein, and neither RGZ ($p = 0.55$ for the main effect of RGZ; Fig. 4*A*) nor p38α MAPK knockdown ($p = 0.10$ for the main effect of p38α MAPK siRNA; Fig. 4*A*) significantly altered PPARγ expression. Furthermore, p38α MAPK siRNA silencing significantly inhibited RGZ-induced expression of *CD36*, *CYP1A1*, and *FABP4*, three PPARγ target genes ($p < 0.001$ for all three genes, RGZ *versus* RGZ plus p38α MAPK siRNA; Fig. 4*B*). Similar to effects in a PPARγ reporter system (Fig. 1*F*), significant interactions between RGZ and p38 MAPK knockdown were seen for *CD36* ($p < 0.001$), *CYP1A1* ($p = 0.04$), and *FABP4* ($p = 0.02$). Table 1 shows all interactions

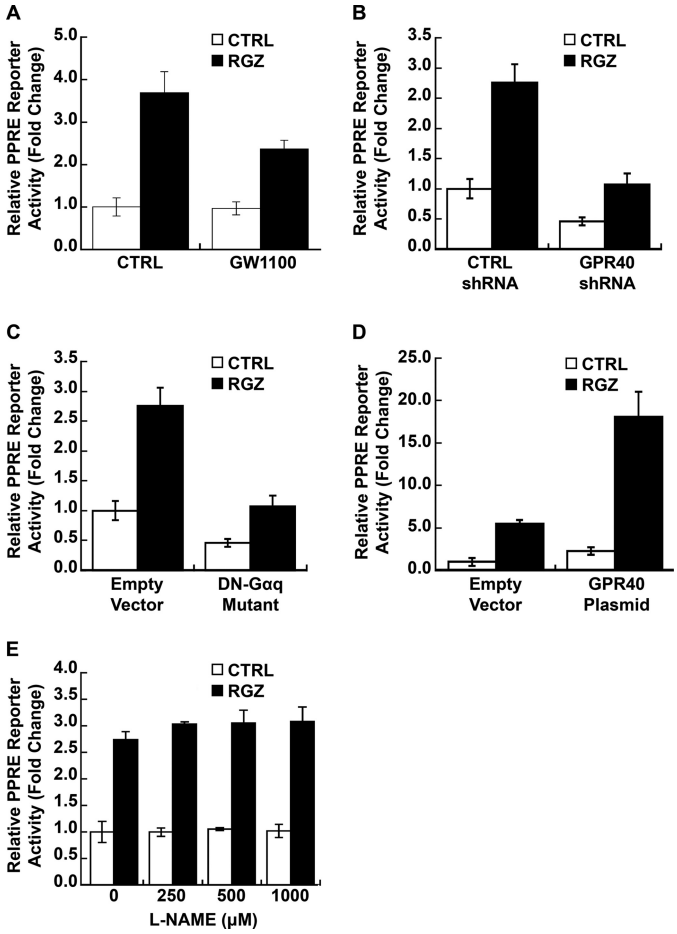

FIGURE 3. **RGZ induces PPRE-driven transcription through GPR40.** *A*, GW1100, a specific GPR40 antagonist, blocked RGZ-induced PPARγ reporter gene activity in EA.hy926 cells ($p < 0.001$ for RGZ *versus* GW1100 plus RGZ). GW1100 (20 μM) or vehicle CTRL was added 40 min before RGZ (10 μM) or its vehicle CTRL. GPR40 shRNA knockdown (*B*) and expression of a $G\alpha_q$ dominant negative mutant (*DN-*$G\alpha_q$) (*C*) inhibited both basal and RGZ-induced PPARγ reporter gene activity in EA.hy926 cells ($p < 0.001$ for GPR40 shRNA main effect in *B*; $p < 0.001$ for DN-$G\alpha_q$ main effect in *C*). *D*, GPR40 overexpression increased both basal and RGZ-induced PPARγ reporter gene activity in EA.hy926 cells ($p < 0.001$ for GPR40 plasmid main effect). *E*, L-NAME, a nitric-oxide synthase inhibitor, did not affect RGZ-induced PPARγ reporter gene activity in EA.hy926 cells ($p = 0.25$ for the main effect of L-NAME). L-NAME (0–1 mM) was added 1 h before RGZ (10 μM) or its CTRL. EA.hy926 cells were co-transfected with PPRE-LUC reporter and $PPAR\gamma_2$ expression plasmid with or without specific GPR40 shRNA, CTRL shRNA, a DN-$G\alpha_q$ plasmid, a GPR40 expression plasmid, or the appropriate control empty vector, as indicated. At 48 h after transfection, cells were treated with RGZ (10 μM) or vehicle CTRL for 24 h prior to the measurement of luciferase activity. Results are presented as means ± S.E. (*error bars*) of independent experiments in *A–D* ($n = 5$) and *E* ($n = 3$).

(*p* values) between RGZ activation of PPARγ and siRNA silencing of GPR40 pathway components on the expression of these target genes in PAECs.

Like EA.hy926 cells, PAECs also express GPR40 as measured by Western blotting, and RGZ did not alter this expression ($p = 0.30$ for the main effect of RGZ; Fig. 4*C*). GPR40 siRNA significantly reduced GPR40 protein expression ($p = 0.002$ for the main effect of GPR40 siRNA; Fig. 4*C*) but had no effect on PPARγ expression in PAECs ($p = 0.56$ for the main effect of GPR40 siRNA; Fig. 4*C*). Similar to p38α MAPK knockdown, GPR40 siRNA significantly blocked the RGZ-induced PPARγ target genes *CD36*, *CYP1A1*, and *FABP4* ($p \leq 0.005$ for all three genes, RGZ *versus* RGZ plus GPR40 siRNA; Fig. 4*D*). Again, RGZ and GPR40 siRNA silencing appeared to interact at endogenous PPARγ target genes (Fig. 4*D* and Table 1). This was in contrast to the additive effects of RGZ and GPR40, knockdown, DN-$G\alpha_q$ mutant, or overexpression on a PPARγ reporter (Fig. 3). PAEC donor, passage number, and day of experiment varied between Fig. 4, *B* and *D*, possibly accounting for the observed variability in gene expression among the siRNA control conditions. These results further support the existence of a functional pathway in endothelial cells that connects GPR40 on the cell surface to nuclear PPARγ signaling, two receptors that can be activated by shared ligands.

PGC1α Transduces RGZ/GPR40/p38 MAPK Signals to PPARγ in PAECs—PGC1α is an essential co-activator of PPARγ. Activated p38 MAPK phosphorylates PGC1α and thereby activates and stabilizes PGC1α protein (18, 19, 48, 49). Therefore, we investigated the role of PGC1α in transducing GPR40/p38 MAPK signals to PPARγ in human PAECs. RGZ induced PGC1α phosphorylation ($p = 0.001$ for RGZ *versus* control within the control siRNA condition; Fig. 5*A*), and siRNA knockdown of either p38α MAPK ($p = 0.45$) or GPR40 abolished this effect ($p = 0.60$; Fig. 5*A*). RGZ also increased total PGC1α protein expression in PAECs ($p = 0.01$ within control siRNA; Fig. 5*B*), an effect that was similarly blocked by either p38α MAPK or GPR40 siRNA silencing ($p \geq 0.62$ for both; Fig. 5*B*). Notably, RGZ increased total and phosphorylated PGC1α without altering their ratio (Fig. 5, *A* and *B*), and both effects may have contributed to PPARγ transcriptional activation.

In contrast to the activation of PGC1α by p38 MAPK-mediated phosphorylation, acetylation inhibits PGC1α activity and therefore also plays a key regulatory role in the co-transcriptional activity of PGC1α (24, 25). SIRT1 binds to and deacetylates PGC1α both *in vivo* and *in vitro* and appears to be required for PGC1α activation (24, 25). Therefore, we evaluated the role of SIRT1 in RGZ/GPR40/p38 MAPK/PGC1α PPARγ signal transduction. RGZ decreased PGC1α acetylation in PAECs ($p < 0.001$ for RGZ *versus* control within the control siRNA condition; Fig. 5*C*), whereas SIRT1-specific siRNA increased PGC1α acetylation ($p < 0.001$ for SIRT1 siRNA *versus* control siRNA in the absence and presence of RGZ; Fig. 5*C*) and abolished the decrease in PGC1α acetylation seen with RGZ ($p = 0.37$ for RGZ *versus* control within the SIRT1 siRNA condition; Fig. 5*C*).

As expected and consistent with the importance of PGC1α as a PPARγ transcriptional co-activator, siRNA silencing of either PGC1α or SIRT1 significantly inhibited RGZ-induced PPARγ target genes (Fig. 5*D*, *left* and *right panels*, respectively) including *CD36*, *CYP1A1*, and *FABP4* ($p < 0.001$ for all three genes, RGZ *versus* RGZ plus PGC1α or SIRT1 siRNA; Fig. 5*D*). As seen for p38 MAPK and GPR40 knockdown, the silencing of either PGC1α or SIRT1 profoundly reduced the ability of RGZ to induce PPARγ target genes (Fig. 5*D* and Table 1). Specific siRNA for PGC1α and SIRT1 effectively reduced PGC1α ($p = 0.001$ for the main effect of PGC1α siRNA; Fig. 5*E*) and SIRT1 ($p < 0.001$ for the main effect of SIRT1 siRNA; Fig. 5*F*) protein

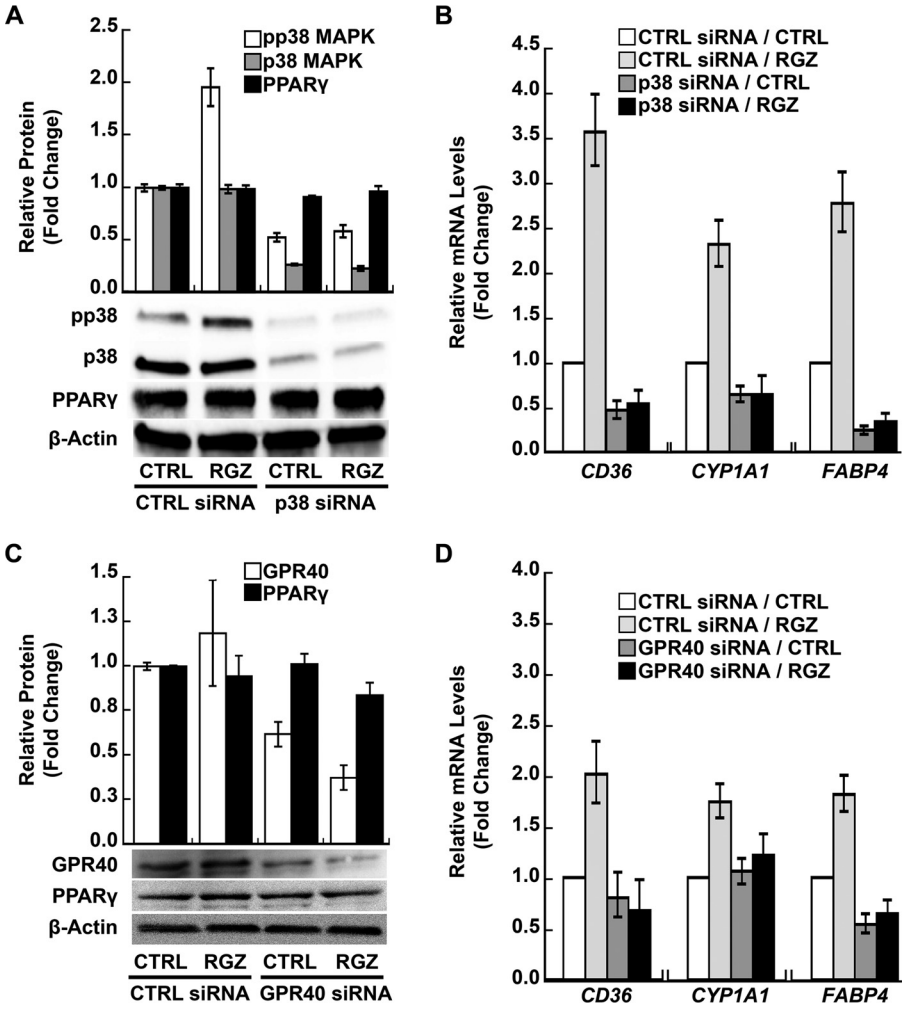

FIGURE 4. **RGZ induces PPARγ target genes through GPR40 and the downstream activation of p38 MAPK in PAECs.** *A*, RGZ-induced p38α MAPK phosphorylation ($p < 0.001$ for RGZ *versus* CTRL within the CTRL siRNA condition). Knockdown of p38α MAPK blocked RGZ-induced p38 MAPK phosphorylation ($p = 0.43$ for RGZ *versus* CTRL within the p38α siRNA condition; $p = 0.009$ for an interaction between p38 MAPK siRNA and RGZ) and decreased total p38 MAPK protein ($p < 0.001$ for p38α siRNA main effect) but did not alter PPARγ protein expression ($p = 0.10$ for p38α siRNA main effect). *B*, p38α MAPK siRNA silencing significantly inhibited RGZ-induced expression of PPARγ target genes ($p < 0.001$ for RGZ *versus* RGZ plus p38α siRNA for all three genes); *C*, GPR40 siRNA knockdown reduced GPR40 protein expression ($p = 0.002$ for GPR40 siRNA main effect) without affecting PPARγ expression ($p = 0.56$ for GPR40 siRNA main effect). *D*, GPR40 siRNA knockdown suppressed RGZ-induced PPARγ target genes ($p \leq 0.005$, RGZ *versus* RGZ plus GPR40 siRNA for all three genes). PAECs were transfected with specific siRNA or a scrambled CTRL siRNA. At 48 h after transfection, cells were treated with RGZ (10 μM) or vehicle CTRL for 30 min prior to the measurement of phosphorylated p38 MAPK (pp38), total p38 MAPK (p38), and PPARγ in *A* and for 24 h prior to the measurement of GPR40 and PPARγ in *C* by Western blotting. In *B* and *D*, 48 h after siRNA transfection, cells were treated with RGZ (10 μM) or vehicle CTRL for 24 h followed by measurement of PPARγ target genes by real-time PCR. Densitometry results of three independent experiments using different PAEC donors and a representative blot are shown in *A* and *C*. In *B* ($n = 5$) and *D* ($n = 4$), results are presented as geometric means ± S.E. (*error bars*) of independent experiments using different PAEC donors.

TABLE 1

The PPARγ agonist RGZ and signaling through the GPR40 pathway function synergistically to induce PPARγ-regulated genes

	p values for RGZ and siRNA silencing interactions			
siRNA target	*CD36*	*CYP1A1*	*FABP4*	All three genes combined
p38 MAPK	<0.001	0.04	0.02	<0.001
GPR40	0.04	0.02	0.11	0.03
PGC1α	0.005	0.18	0.006	0.03
SIRT1	<0.001	0.09	0.06	<0.001
EP300	<0.001	0.007	<0.001	0.008
All siRNA silencing combined	<0.001	0.001	<0.001	<0.001

expression in PAECs, respectively. RGZ did not alter SIRT1 protein expression ($p = 0.83$ for the main effect of RGZ; Fig. 5*F*) or phosphorylation state (data not shown).

EP300 Contributes to the RGZ/GPR40/p38 MAPK/PGC1α/PPARγ Signaling Pathway—EP300, a general transcriptional co-activator with intrinsic histone acetyltransferase and chromatin remodeling activity, has been shown to interact with PGC1α and PPARγ, thereby enhancing PPARγ transcriptional activity (50, 51). Importantly, p38 MAPK has been demonstrated to directly phosphorylate EP300, thereby potentiating its acetyltransferase activity (22, 52). Therefore, the role of EP300 in the pathway described here was investigated in human endothelial cells. Consistent with the role of PGC1α in PPARγ signaling, PGC1α overexpression in EA.hy926 cells increased PPRE reporter activity ($p < 0.001$ for a plasmid dose effect in the absence of RGZ; Fig. 6*A*). A similar dose response was seen in the presence of RGZ, but the RGZ effect became smaller with increasing amounts of PGC1α plasmid ($p < 0.001$ for a negative interaction between RGZ and PGC1α; Fig. 6*A*), possibly

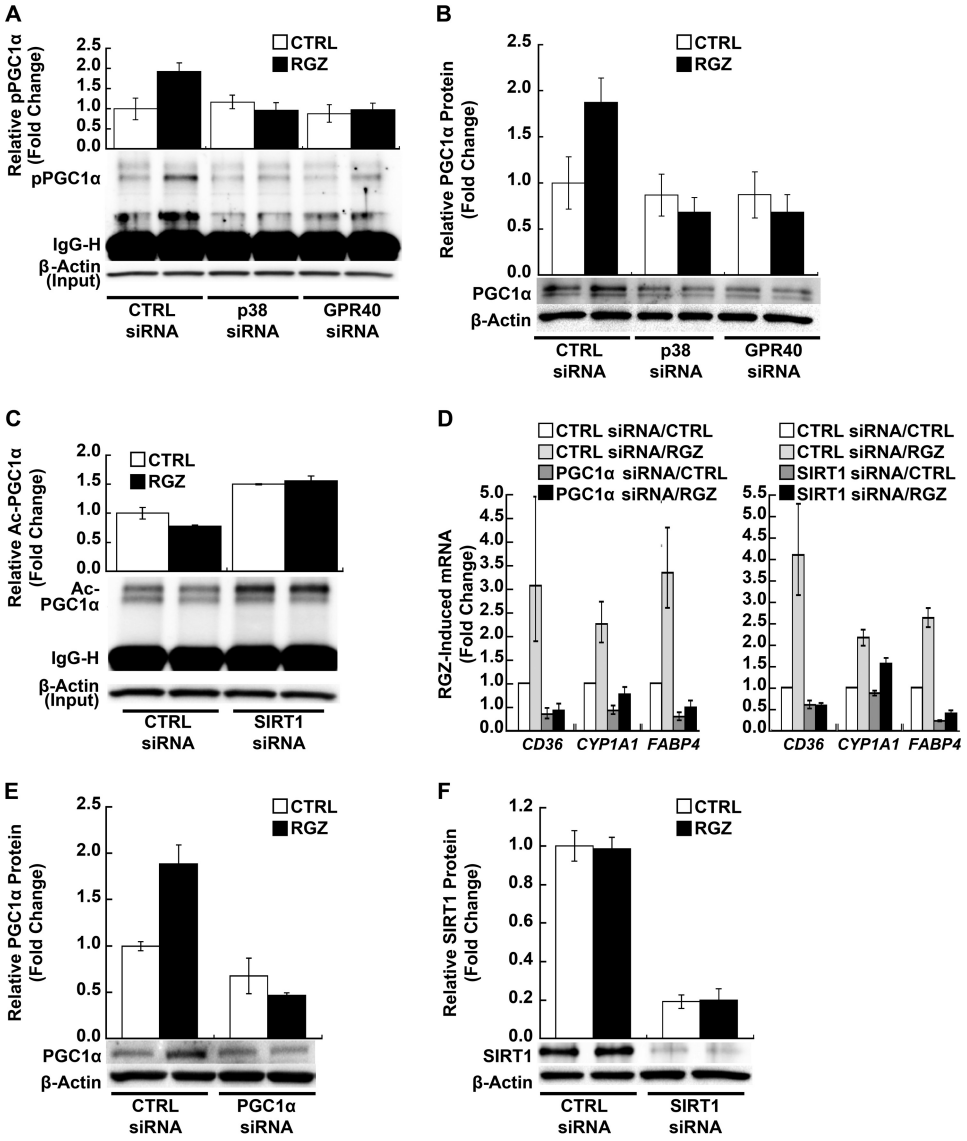

FIGURE 5. **PGC1α transduces RGZ/GPR40/p38 MAPK signaling to PPARγ in PAECs.** *A*, RGZ induced PGC1α phosphorylation, an effect blocked by siRNA knockdown of p38α MAPK or GPR40 ($p = 0.001$ for RGZ *versus* CTRL within CTRL siRNA; $p \geq 0.45$, RGZ *versus* CTRL within p38α or GPR40 siRNA conditions). PAECs were transfected with specific siRNA or scrambled CTRL siRNA, as indicated. At 48 h after transfection, cells were treated with RGZ (10 μM) or vehicle CTRL for 1 h prior to the extraction of nuclear protein for immunoprecipitation with phosphothreonine and phosphoserine antibodies. Phospho-PGC1α (*pPGC1α*) in immunoprecipitates was detected by Western blotting with anti-PGC1α. *B*, RGZ induced PGC1α protein expression in PAECs, an effect blocked by siRNA knockdown of p38α MAPK or GPR40 ($p = 0.01$ for RGZ *versus* CTRL within CTRL siRNA; $p \geq 0.62$, RGZ *versus* CTRL within p38α or GPR40 siRNA). Cells were transfected as in *A*. At 48 h after transfection, cells were treated with RGZ (10 μM) or vehicle CTRL for 4 h prior to the extraction of nuclear protein for measurement of PGC1α by Western blotting. *C*, RGZ slightly decreased ($p < 0.001$ for RGZ *versus* CTRL within CTRL siRNA), but SIRT1 siRNA increased PGC1α acetylation in PAECs ($p < 0.001$ for SIRT1 siRNA *versus* CTRL siRNA in the absence and presence of RGZ). At 48 h after transfection, PAECs were treated with RGZ (10 μM) or vehicle CTRL for 4 h prior to the extraction of whole cell lysates for immunoprecipitation with anti-acetyl-lysine antibodies. Acetyl-PGC1α (*Ac-PGC1α*) in immunoprecipitates was detected by Western blotting with anti-PGC1α. *D*, siRNA knockdown of PGC1α or SIRT1 inhibited RGZ-induced PPARγ target genes in PAECs ($p < 0.001$ for RGZ *versus* RGZ plus PGC1α or SIRT1 siRNA for *CD36*, *CYP1A1*, and *FABP4*). Results are presented as geometric means ± S.E. (*error bars*) of five independent experiments using different PAEC donors. *E* and *F*, specific siRNA for PGC1α and SIRT1 reduced their protein expression in PAECs, respectively ($p \leq 0.001$, main effects of PGC1α and SIRT1 siRNA). Cells were transfected with siRNA for PGC1α or SIRT1 or scrambled CTRL siRNA. At 48 h after transfection, PAECs were treated with RGZ (10 μM) or vehicle CTRL for 24 h prior to isolation of total RNA for measurement of PPARγ target genes by real-time PCR or for 4 h prior to the preparation of nuclear protein or whole cell lysates for measurement of PGC1α and SIRT, respectively, by Western blotting. Densitometry results of independent experiments using different PAEC donors (*top panels*) and a representative blot (*bottom panels*) are shown in *A* and *B* ($n = 4$), *C* ($n = 5$), *E* ($n = 3$), and *F* ($n = 4$).

because RGZ/p38 MAPK-dependent induction and phosphorylation of PGC1α was rendered less important by direct PGC1α overexpression.

EP300 overexpression also increased both basal and RGZ-induced PPRE reporter activity ($p = 0.003$ for EP300 main effect; $p = 0.68$ for an interaction between EP300 and RGZ; Fig. 6*B*). Although PGC1α overexpression had a stronger overall effect on PPRE reporter activity ($p < 0.02$ for PGC1α *versus* EP300 in both the absence and presence of RGZ; Fig. 6*C*), EP300 overexpression better preserved RGZ effect size and increased PPRE reporter activity additively with PGC1α in the presence of RGZ ($p < 0.001$ for PGC1α and EP300 main effects; $p = 0.77$ for an interaction between PGC1α and EP300; Fig. 6*C*). Notably, RGZ treatment of EA.hy926 cells increased EP300

phosphorylation in EA.hy926 cells ($p = 0.01$ for RGZ *versus* control within the control condition; Fig. 6*D*), an activating event blocked by either p38 MAPK (SB) or GPR40 (GW1100) inhibition ($p \geq 0.19$ for RGZ *versus* control in the presence of SB or GW1100; Fig. 6*D*). Specific siRNA silencing of EP300 inhibited both basal and RGZ-induced PPRE reporter activity in EA.hy926 cells ($p < 0.001$ for EP300 siRNA main effect; $p = 0.53$ for an interaction between EP300 siRNA and RGZ; Fig. 6*E*). Likewise, siRNA knockdown of EP300 in PAECs significantly inhibited RGZ-induced PPARγ target genes, *CD36*, *CYP1A1*, and *FABP4* ($p < 0.001$ for all three, RGZ *versus* RGZ plus EP300 siRNA; Fig. 6*F*). Similar to the knockdown of other GPR40 pathway components, EP300 silencing markedly interfered with the ability of RGZ/PPARγ signaling to induce *CD36*, *CYP1A1*, and *FABP4* (Fig. 6*F* and Table 1). Efficient knockdown of *EP300* mRNA expression was

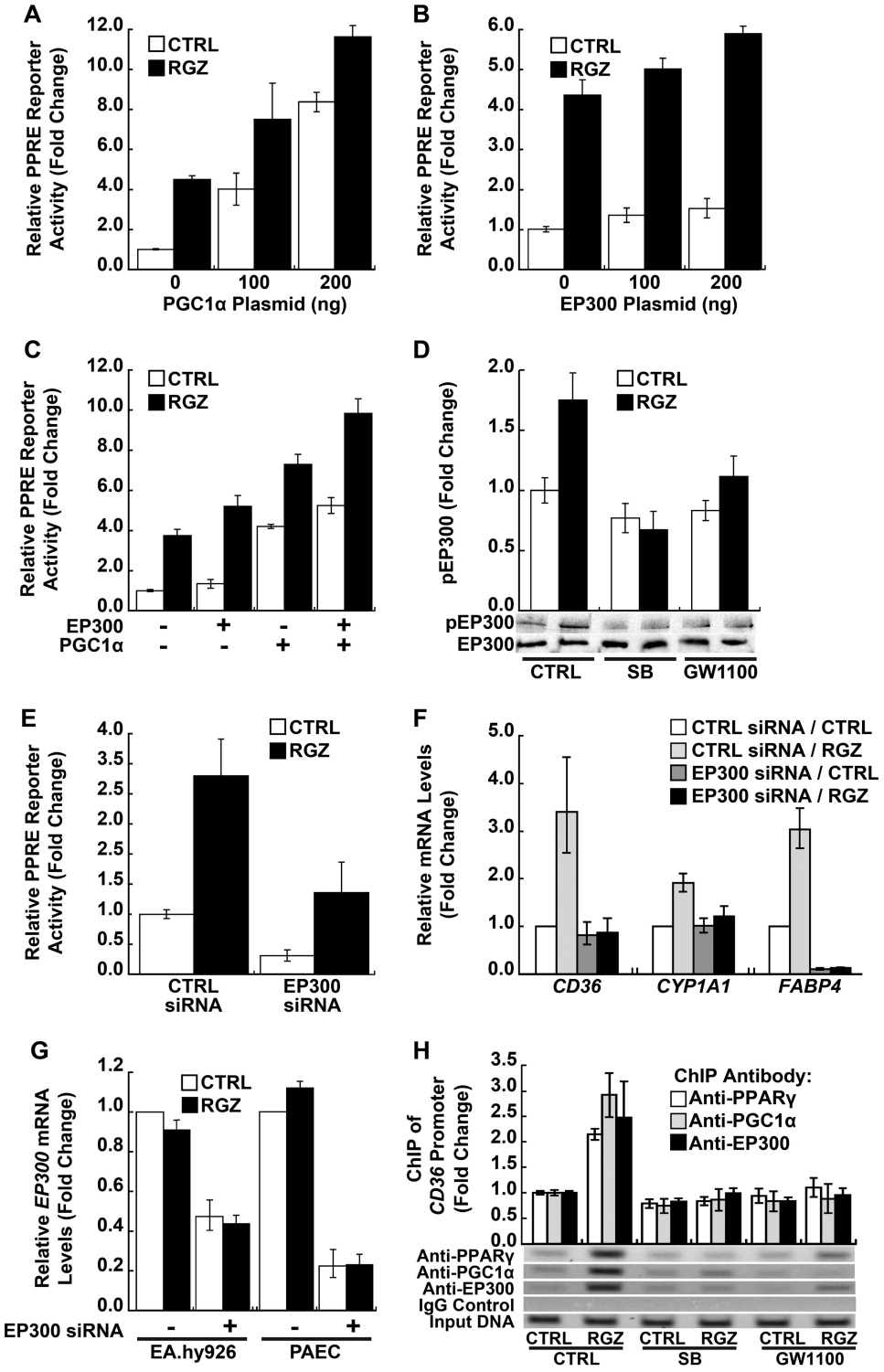

achieved in both EA.hy926 cells and PAECs ($p < 0.001$ for both; Fig. 6*G*).

RGZ-induced Binding of PPARγ, PGC1α, and EP300 to the Proximal CD36 Promoter; Dependence on p38 MAPK and GPR40—PGC1α and EP300 remodel and open chromatin for active transcription. Therefore, RGZ/GPR40/p38 MAPK signaling may be critical for certain genes and in some cell types for PPARγ transcriptional activation. ChIP assays in human PAECs demonstrated that RGZ increased the binding of endogenous PPARγ ($p < 0.001$), PGC1α ($p = 0.004$), and EP300 ($p = 0.04$) to native PPREs in the proximal *CD36* promoter (comparing RGZ with control in the absence of SB or GW1100; Fig. 6*H*). These effects on PPARγ, PGC1α, and EP300 binding were all abolished by either p38 MAPK (SB) or GPR40 (GW1100) inhibition ($p \geq 0.18$ for RGZ *versus* control in the presence of SB or GW1100; $p \leq 0.03$ for interactions between RGZ and SB or GW1100 on the binding of PPARγ, PGC1α, and EP300; Fig. 6*H*).

Discussion

Our results demonstrate that GPR40 and PPARγ can function together as an integrated two-receptor signal transduction pathway. Besides the direct activation of its canonical receptor PPARγ, RGZ also required GPR40 to optimally propagate a PPARγ nuclear signal in human endothelium (Fig. 7). GPR40 and PPARγ appeared to function at least additively and sometimes synergistically to initiate PPARγ genomic responses, depending on the transcriptional context. This conclusion is based on the following: 1) RGZ activated p38 MAPK; 2) PPARγ DNA binding and reporter activity was at least partially p38 MAPK-dependent; 3) GPR40 inhibition or knockdown blocked RGZ activation of p38 MAPK; 4) inhibition of GPR40 signaling, including use of an antagonist, GPR40 silencing, or expression of a DN-$G\alpha_q$ mutant, suppressed, whereas GPR40 overexpression further increased, RGZ-induced PPRE reporter activity; 5) RGZ activation of p38 MAPK and the PPRE reporter was independent of •NO synthase, and •NO activation of p38 MAPK was likewise GPR40-independent; and importantly, 6) in human primary PAECs, knockdown of p38 MAPK or GPR40 substantially reduced the ability of RGZ to induce PPARγ target genes.

In addition to these findings, RGZ treatment of PAECs increased the phosphorylation and expression of PGC1α, a key co-activator of PPARγ (50). Knockdown of either p38α MAPK or GPR40 abolished these effects of RGZ on PGC1α. RGZ also modestly decreased PGC1α acetylation, an activating event; knockdown of SIRT1, a deacetylase, eliminated this effect and increased PGC1α acetylation. As expected, given its essential role in the formation of a PPARγ transcriptional activation complex (50), knockdown of PGC1α or its essential activator SIRT1 inhibited RGZ-induced PPARγ target gene expression in PAECs. Finally, EP300, an acetylase that docks with PGC1α and remodels chromatin to optimize the transcription of PPARγ target genes (50, 53), was also phosphorylated and activated by p38 MAPK. Like PGC1α, EP300 appeared to play an important downstream role in RGZ/GPR40/p38 MAPK modulation of PPARγ signaling. Collectively, these experiments demonstrate that p38 MAPK, PGC1α, and EP300 link GPR40 to downstream PPARγ genomic signaling. Binding to and activating both GPR40 and PPARγ appears to be a common feature of several PPARγ agonists (29–34). This direct connection between GPR40 signaling and PPARγ transcriptional activation argues that the effects of these ligands on human endothelium might be best understood as a cognate two-receptor system, integrated by p38 MAPK, PGC1α, and EP300.

Activation of p38 MAPK increases transcription of PPARγ-regulated genes in endothelial cells (39) and adipocytes (20, 21, 54). TZDs (20, 55–57) have been long known to activate p38 MAPK independent of PPARγ in various cell types, including adipocytes, astrocytes, and epithelial cells. However, the potential role of GPR40 was not appreciated at the time of these early studies, and the underlying mechanisms seemed to be cell type-dependent (20, 55–57). Reactive oxygen species were implicated in astrocytes (55) and adipocytes (20), whereas endoplasmic reticulum stress was implicated in liver epithelial cells (57). Here, RGZ activation of p38 MAPK was directly tied to GPR40 in human endothelium. Both the GPR40 antagonist GW1100 and GPR40 gene silencing significantly blocked RGZ-induced p38 MAPK phosphorylation. This finding is consistent with recent reports that TZDs bind to and activate GPR40 in bron-

FIGURE 6. **CBP/EP300 participation in RGZ/GPR40/p38 MAPK/PGC1α/PPARγ signaling.** *A–C*, overexpression of PGC1α, CBP/EP300, or both enhanced PPARγ reporter gene activity. In *A*, PGC1α overexpression increased PPRE reporter activity in the absence of RGZ ($p < 0.001$ for a plasmid dose effect); the PGC1α effect became smaller in the presence of RGZ ($p < 0.001$ for a negative interaction between RGZ and PGC1α). In *B*, EP300 overexpression also increased both basal and RGZ-induced PPRE reporter activity ($p = 0.003$ for the main effect; $p = 0.68$ for an interaction between RGZ and EP300 plasmid). In *C*, PGC1α and EP300 additively enhanced PPRE reporter activity in the absence and presence of RGZ ($p < 0.001$ for PGC1α and EP300 main effects; $p = 0.77$ for an interaction between PGC1α and EP300). EA.hy926 cells were co-transfected with PPRE-LUC reporter; a $PPAR\gamma_2$ expression plasmid; and either a PGC1α expression plasmid, an EP300 expression plasmid, or both, as indicated. DNA amounts were balanced with the empty vector pcDNA3.1 plasmid. At 24 h after transfection, cells were treated with RGZ (10 μM) or vehicle CTRL for 24 h prior to the measurement of luciferase activity. *D*, RGZ induced EP300 phosphorylation in EA.hy926 cells ($p = 0.01$ for RGZ *versus* CTRL within CTRL), an effect blocked by SB, a specific p38 MAPK inhibitor, or GW1100, a specific GPR40 antagonist ($p \geq 0.19$ for RGZ *versus* CTRL with SB or GW1100). Cells were treated with SB (10 μM), GW1100 (20 μM), or vehicle CTRL for 40 min and then incubated with RGZ (10 μM) or vehicle CTRL for another 15 min prior to the extraction of whole cell lysates for measurement of phosphorylated and total EP300 by Western blotting. Densitometry results of three independent experiments and a representative blot are shown. *E*, siRNA knockdown of EP300 inhibited PPARγ reporter gene activity ($p < 0.001$ for EP300 siRNA main effect; $p = 0.53$ for an interaction between EP300 siRNA and RGZ). EA.hy926 cells were first transfected with EP300 siRNA or scrambled CTRL siRNA for 48 h and then co-transfected with PPRE-LUC reporter and a $PPAR\gamma_2$ expression plasmid for 24 h, followed by an additional 24-h treatment of RGZ (10 μM) or vehicle CTRL prior to the measurement of luciferase activity. *F*, EP300 siRNA inhibited RGZ-induced PPARγ target genes ($p < 0.001$ for RGZ *versus* RGZ plus EP300 siRNA for all three genes) in PAECs. *G*, EP300 siRNA reduced *EP300* mRNA in EA.hy926 cells and PAECs ($p < 0.001$ for the main effect of EP300 siRNA in both cell types). Cells were transfected with EP300 siRNA or scrambled CTRL siRNA for 48 h and then treated with RGZ (10 μM) or vehicle CTRL for 24 h prior to isolation of total RNA for measurement of PPARγ target genes and *EP300* mRNA by real-time PCR. *H*, RGZ increased the binding of PPARγ ($p < 0.001$), PGC1α ($p = 0.004$), and EP300 ($p = 0.04$) to PPRE in the *CD36* promoter (RGZ *versus* CTRL within the CTRL condition), an effect blocked by SB or GW1100 ($p \geq 0.18$, RGZ *versus* CTRL for both inhibitors and all three proteins). PAECs were treated with SB (10 μM), GW1100 (20 μM), or vehicle control (CTRL) for 40 min and then incubated with RGZ (10 μM) or vehicle CTRL for another 24 h prior to ChIP assay with anti-PPARγ, anti-PGC1α, anti-EP300, or control IgG. Densitometry measurements were normalized to input DNA. Representative PCR results are shown for each pull-down. *Panels* represent the results of three (*A–F*) or four (*G* and *H*) independent experiments. For PAECs, different donors were used in performing replicates. *Error bars*, S.E.

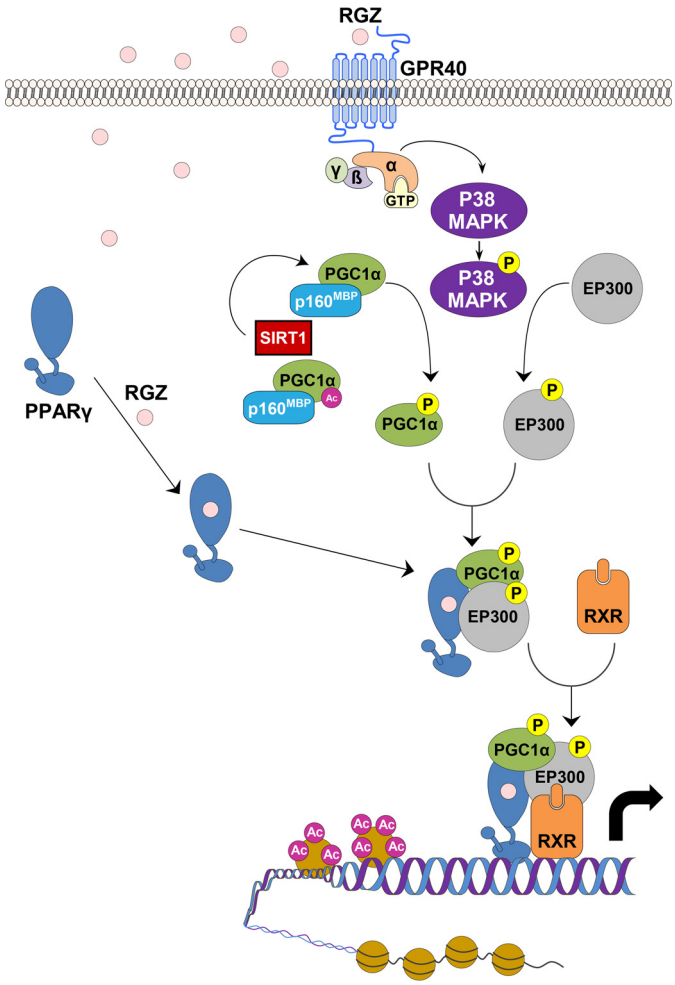

FIGURE 7. **Proposed GPR40 and PPARγ integrated signal transduction pathway in human endothelial cells.** In the classical PPARγ signaling pathway, RGZ binds directly to PPARγ, inducing a conformational change that results in its dissociation from co-repressors (not depicted), such as nuclear co-repressor and histone deacetylases, and the recruitment of co-activators, including PGC1α and EP300. However, as shown here, RGZ and other PPARγ ligands also bind to and activate GPR40 on the cell surface, resulting in p38 MAPK phosphorylation, which in turn phosphorylates and thereby activates both PGC1α and EP300. As noted, PGC1α deacetylation by SIRT1 is also essential for its activation. Phosphorylation releases PGC1α from its repressor $p160^{MBP}$ and leads to a conformational change, permitting PGC1α to dock with PPARγ and recruit newly activated EP300. EP300 is a histone acetyltransferase that remodels local chromatin and enhances gene transcription. The activated PPARγ complex thus heterodimerizes with retinoid X receptor, which binds to peroxisome proliferator response elements in accessible promoters, inducing the transcription of target genes.

chial epithelial cells (32), osteocytes (33), and GPR40-transfected HEK293 cells (31, 58), causing the rapid phosphorylation of p38 MAPK (31, 33, 58).

As already noted, p38 MAPK has been shown to phosphorylate the PPARγ co-activator PGC1α (18–21). Phosphorylation disrupts PGC1α binding to its repressor, p160 Myb-binding protein ($p160^{MBP}$), freeing it to dock with PPARγ (19, 53). Docking with PPARγ changes the conformation of PGC1α and allows binding of EP300, a histone acetyltransferase essential for PGC1α/PPARγ-dependent gene transcription (19, 50, 53, 59). Moreover, p38 MAPK phosphorylation of PGC1α increases its half-life (18). Furthermore, the p38 MAPK/ATF2 pathway induces PGC1α mRNA transcription (48, 49), increasing PGC1α protein expression and further enhancing PGC1α/PPARγ-mediated gene transcription. In addition to PGC1α, p38 MAPK also phosphorylates EP300, potentiating its histone acetyltransferase activity (22, 52), an additional mechanism by which p38 MAPK contributes to the transcriptional activation of PPARγ. Consistent with these previous findings, PGC1α and EP300 were shown here to connect RGZ/GPR40/p38 MAPK transmembrane signaling to the downstream transcriptional activation of RGZ/PPARγ in the cell nucleus.

Like phosphorylation, reversible acetylation is another key modulator of PGC1α (24, 25). So far, only two proteins have been unequivocally shown to regulate the reversible acetylation of PGC1α, the acetyltransferase GCN5 (23) and the NAD^+-dependent deacetylase SIRT1 (24, 25). GCN5 acetylates and inhibits PGC1α activity (23), whereas SIRT1 deacetylates and enhances PGC1α activity and in turn induces transcription of its target genes (24, 25). Overexpression of Sirt1 in the liver of mice induces gluconeogenic genes under the control of PGC1α, whereas Sirt1 knockdown attenuates this effect (60). Also, in skeletal muscle, Sirt1 is required for PGC1α-mediated induction of the fatty acid oxidation pathway (61). In the present study, RGZ was seen to modestly decrease PGC1α acetylation in endothelial cells; SIRT1 knockdown eliminated this effect, increasing PGC1α acetylation. These results suggest that PGC1α phosphorylation might facilitate its deacetylation by SIRT1. It was previously reported that JNK1 phosphorylates SIRT1 and promotes its enzymatic activity in HEK293T cells (62); p38 MAPK has been reported to increase SIRT1 expression in neurons (63) and decrease it in chondrocytes (64). In our study, RGZ did not affect either SIRT1 phosphorylation or expression in endothelial cells. However, consistent with its essential role in activating PGC1α via deacetylation, SIRT1 knockdown significantly inhibited RGZ-induced PPARγ target gene expression in endothelial cells.

Although the effects of RGZ/PPARγ and RGZ/GPR40 were mostly additive in PPRE reporter assays, the dual activation of both receptors appeared interdependent and synergistic at PPARγ-regulated target genes in the chromatin microenvironment (see Table 1 for a summary of interactions between RGZ and GPR40 pathway siRNA silencing). Across all three PPARγ-regulated genes combined, interaction testing between RGZ and each siRNA target indicated that RGZ activation of GPR40 and PPARγ function synergistically (Table 1). Likewise, across all siRNA silencing combined, each PPARγ-regulated gene, *CD36* ($p < 0.001$), *CYP1A1* ($p = 0.001$) and *FABP4* ($p < 0.001$), demonstrated significant interactions between RGZ-induced PPARγ responses and signaling through the GPR40 pathway (Table 1). Largely additive effects on a PPRE reporter plasmid and evidence for GPR40 and PPARγ interdependence at endogenous genes might be explained by the ability of the proposed signaling cascade to actively remodel chromatin. Consistent with this concept, p38 MAPK or GPR40 inhibition both markedly blocked the RGZ-induced binding of PPARγ, PGC1α, and EP300 to a PPRE-rich site in the proximal promoter of *CD36*, a prototypic PPARγ target gene.

TZDs, synthetic ligands of PPARγ, including RGZ, ciglitazone, troglitazone, and pioglitazone, have all been shown to activate GPR40 with subsequent signal transduction through stress kinases (29–34). RGZ compared with pioglitazone (two

TZDs used to treat type 2 diabetes mellitus) produces a more potent and prolonged activation of ERK1/2 (31), a stress kinase pathway associated with vascular inflammation (65). These differences in the potency and sustainability of ERK1/2 activation could potentially explain some of the efficacy and safety differences among existing synthetic PPARγ ligands. Different from TZDs, 15-deoxy-Δ12,14-prostaglandin J2, a natural PPARγ ligand (27), did not appear to activate GPR40 in bronchial epithelial cells (32). Conversely, agonists selective for GPR40 have been described with little or no effect on PPARγ activity (29, 66). Therefore, it may be possible to design drugs that activate PPARγ independently of GPR40 or selectively activate GPR40/p38 MAPK while circumventing GPR40/ERK activation. Such selective agents or biased ligands (67, 68) might arguably be less inflammatory and thus have better risk/benefit profiles in patients with vascular disease. In addition, unexplored effects through other unidentified cognate GPR and nuclear receptor pairs, as exemplified by GPR40/PPARγ, could explain important safety and efficacy differences among nuclear receptor-directed drugs.

Author Contributions—S. W. and R. L. D. conceived the study, designed experiments, analyzed and interpreted data, and wrote the paper. S. W. performed transfections, Western blots, PPARγ target gene real-time PCR experiments, and the chromatin immunoprecipitation assays. K. S. A. identified the role played by EP300, helped design key experiments related to acetylation, maintained the pulmonary artery endothelial cell cultures, and revised drafts of the manuscript. J. M. E., E. J. D., and G. A. F. contributed to the scientific concept, provided technical advice, raised critical questions, and revised drafts of the manuscript. E. J. D. also lent important expertise in nuclear receptor signaling. J. Y. W. performed the experiments shown in Fig. 2, *B–D*. A. P. started the study and performed the experiments shown in Fig. 1. R. C. and J. S. performed the statistical analyses. All authors read, edited, and approved the final version of the manuscript.

Acknowledgments—We thank Drs. Ronald M. Evans and Ae-Kyung Yi for kindly sharing plasmids and Kai Ge for providing the HeLaS/F-PPARγ cell line. We also appreciate the help of Kelly Byrne in editing and formatting the manuscript and figures.

References

1. Buse, J. B., Ginsberg, H. N., Bakris, G. L., Clark, N. G., Costa, F., Eckel, R., Fonseca, V., Gerstein, H. C., Grundy, S., Nesto, R. W., Pignone, M. P., Plutzky, J., Porte, D., Redberg, R., Stitzel, K. F., and Stone, N. J., American Heart Association, and American Diabetes Association (2007) Primary prevention of cardiovascular diseases in people with diabetes mellitus: a scientific statement from the American Heart Association and the American Diabetes Association. *Circulation* **115,** 114–126
2. Yki-Järvinen, H. (2004) Thiazolidinediones. *N. Engl. J. Med.* **351,** 1106–1118
3. McGuire, D. K., and Inzucchi, S. E. (2008) New drugs for the treatment of diabetes mellitus: part I: thiazolidinediones and their evolving cardiovascular implications. *Circulation* **117,** 440–449
4. Ketsawatsomkron, P., Pelham, C. J., Groh, S., Keen, H. L., Faraci, F. M., and Sigmund, C. D. (2010) Does peroxisome proliferator-activated receptor-γ (PPARγ) protect from hypertension directly through effects in the vasculature? *J. Biol. Chem.* **285,** 9311–9316
5. Goldberg, R. B., Kendall, D. M., Deeg, M. A., Buse, J. B., Zagar, A. J., Pinaire, J. A., Tan, M. H., Khan, M. A., Perez, A. T., Jacober, S. J., and GLAI Study Investigators (2005) A comparison of lipid and glycemic effects of pioglitazone and rosiglitazone in patients with type 2 diabetes and dyslipidemia. *Diabetes Care* **28,** 1547–1554
6. Wang, N., Verna, L., Chen, N. G., Chen, J., Li, H., Forman, B. M., and Stemerman, M. B. (2002) Constitutive activation of peroxisome proliferator-activated receptor-γ suppresses pro-inflammatory adhesion molecules in human vascular endothelial cells. *J. Biol. Chem.* **277,** 34176–34181
7. Erdmann, E., Spanheimer, R., Charbonnel, B., and PROactive Study Investigators (2010) Pioglitazone and the risk of cardiovascular events in patients with Type 2 diabetes receiving concomitant treatment with nitrates, renin-angiotensin system blockers, or insulin: results from the PROactive study (PROactive 20). *J. Diabetes* **2,** 212–220
8. Hansmann, G., de Jesus Perez, V. A., Alastalo, T. P., Alvira, C. M., Guignabert, C., Bekker, J. M., Schellong, S., Urashima, T., Wang, L., Morrell, N. W., and Rabinovitch, M. (2008) An antiproliferative BMP-2/PPARγ/apoE axis in human and murine SMCs and its role in pulmonary hypertension. *J. Clin. Invest.* **118,** 1846–1857
9. Reddy, R. C., Narala, V. R., Keshamouni, V. G., Milam, J. E., Newstead, M. W., and Standiford, T. J. (2008) Sepsis-induced inhibition of neutrophil chemotaxis is mediated by activation of peroxisome proliferator-activated receptor-γ. *Blood* **112,** 4250–4258
10. Kahn, B. B., and McGraw, T. E. (2010) Rosiglitazone, PPARγ, and type 2 diabetes. *N. Engl. J. Med.* **363,** 2667–2669
11. Spiegelman, B. M. (1998) PPAR-γ: adipogenic regulator and thiazolidinedione receptor. *Diabetes* **47,** 507–514
12. Pascual, G., Fong, A. L., Ogawa, S., Gamliel, A., Li, A. C., Perissi, V., Rose, D. W., Willson, T. M., Rosenfeld, M. G., and Glass, C. K. (2005) A SUMOylation-dependent pathway mediates transrepression of inflammatory response genes by PPAR-γ. *Nature* **437,** 759–763
13. Hu, E., Kim, J. B., Sarraf, P., and Spiegelman, B. M. (1996) Inhibition of adipogenesis through MAP kinase-mediated phosphorylation of PPARγ. *Science* **274,** 2100–2103
14. Adams, M., Reginato, M. J., Shao, D., Lazar, M. A., and Chatterjee, V. K. (1997) Transcriptional activation by peroxisome proliferator-activated receptor γ is inhibited by phosphorylation at a consensus mitogen-activated protein kinase site. *J. Biol. Chem.* **272,** 5128–5132
15. Camp, H. S., and Tafuri, S. R. (1997) Regulation of peroxisome proliferator-activated receptor γ activity by mitogen-activated protein kinase. *J. Biol. Chem.* **272,** 10811–10816
16. Rangwala, S. M., Rhoades, B., Shapiro, J. S., Rich, A. S., Kim, J. K., Shulman, G. I., Kaestner, K. H., and Lazar, M. A. (2003) Genetic modulation of PPARγ phosphorylation regulates insulin sensitivity. *Dev. Cell* **5,** 657–663
17. Choi, J. H., Banks, A. S., Estall, J. L., Kajimura, S., Boström, P., Laznik, D., Ruas, J. L., Chalmers, M. J., Kamenecka, T. M., Blüher, M., Griffin, P. R., and Spiegelman, B. M. (2010) Anti-diabetic drugs inhibit obesity-linked phosphorylation of PPARγ by Cdk5. *Nature* **466,** 451–456
18. Puigserver, P., Rhee, J., Lin, J., Wu, Z., Yoon, J. C., Zhang, C. Y., Krauss, S., Mootha, V. K., Lowell, B. B., and Spiegelman, B. M. (2001) Cytokine stimulation of energy expenditure through p38 MAP kinase activation of PPARγ coactivator-1. *Mol. Cell* **8,** 971–982
19. Fan, M., Rhee, J., St-Pierre, J., Handschin, C., Puigserver, P., Lin, J., Jäeger, S., Erdjument-Bromage, H., Tempst, P., and Spiegelman, B. M. (2004) Suppression of mitochondrial respiration through recruitment of p160 myb binding protein to PGC-1α: modulation by p38 MAPK. *Genes Dev.* **18,** 278–289
20. Teruel, T., Hernandez, R., Benito, M., and Lorenzo, M. (2003) Rosiglitazone and retinoic acid induce uncoupling protein-1 (UCP-1) in a p38 mitogen-activated protein kinase-dependent manner in fetal primary brown adipocytes. *J. Biol. Chem.* **278,** 263–269
21. Cao, W., Daniel, K. W., Robidoux, J., Puigserver, P., Medvedev, A. V., Bai, X., Floering, L. M., Spiegelman, B. M., and Collins, S. (2004) p38 mitogen-activated protein kinase is the central regulator of cyclic AMP-dependent transcription of the brown fat uncoupling protein 1 gene. *Mol. Cell. Biol.* **24,** 3057–3067
22. Bratton, M. R., Frigo, D. E., Vigh-Conrad, K. A., Fan, D., Wadsworth, S., McLachlan, J. A., and Burow, M. E. (2009) Organochlorine-mediated potentiation of the general coactivator p300 through p38 mitogen-activated protein kinase. *Carcinogenesis* **30,** 106–113

23. Lerin, C., Rodgers, J. T., Kalume, D. E., Kim, S. H., Pandey, A., and Puigserver, P. (2006) GCN5 acetyltransferase complex controls glucose metabolism through transcriptional repression of PGC-1α. *Cell Metab.* **3,** 429–438
24. Nemoto, S., Fergusson, M. M., and Finkel, T. (2005) SIRT1 functionally interacts with the metabolic regulator and transcriptional coactivator PGC-1α. *J. Biol. Chem.* **280,** 16456–16460
25. Rodgers, J. T., Lerin, C., Haas, W., Gygi, S. P., Spiegelman, B. M., and Puigserver, P. (2005) Nutrient control of glucose homeostasis through a complex of PGC-1α and SIRT1. *Nature* **434,** 113–118
26. Sohda, T., Mizuno, K., Tawada, H., Sugiyama, Y., Fujita, T., and Kawamatsu, Y. (1982) Studies on antidiabetic agents. I. Synthesis of 5-[4-(2-methyl-2-phenylpropoxy)-benzyl]thiazolidine-2,4-dione (AL-321) and related compounds. *Chem. Pharm. Bull.* **30,** 3563–3573
27. Forman, B. M., Tontonoz, P., Chen, J., Brun, R. P., Spiegelman, B. M., and Evans, R. M. (1995) 15-Deoxy-δ12,14-prostaglandin J2 is a ligand for the adipocyte determination factor PPARγ. *Cell* **83,** 803–812
28. Lehmann, J. M., Moore, L. B., Smith-Oliver, T. A., Wilkison, W. O., Willson, T. M., and Kliewer, S. A. (1995) An antidiabetic thiazolidinedione is a high affinity ligand for peroxisome proliferator-activated receptor γ (PPARγ). *J. Biol. Chem.* **270,** 12953–12956
29. Zhou, C., Tang, C., Chang, E., Ge, M., Lin, S., Cline, E., Tan, C. P., Feng, Y., Zhou, Y. P., Eiermann, G. J., Petrov, A., Salituro, G., Meinke, P., Mosley, R., Akiyama, T. E., Einstein, M., Kumar, S., Berger, J., Howard, A. D., Thornberry, N., Mills, S. G., and Yang, L. (2010) Discovery of 5-aryloxy-2,4-thiazolidinediones as potent GPR40 agonists. *Bioorg. Med. Chem. Lett.* **20,** 1298–1301
30. Kotarsky, K., Nilsson, N. E., Flodgren, E., Owman, C., and Olde, B. (2003) A human cell surface receptor activated by free fatty acids and thiazolidinedione drugs. *Biochem. Biophys. Res. Commun.* **301,** 406–410
31. Smith, N. J., Stoddart, L. A., Devine, N. M., Jenkins, L., and Milligan, G. (2009) The action and mode of binding of thiazolidinedione ligands at free fatty acid receptor 1. *J. Biol. Chem.* **284,** 17527–17539
32. Gras, D., Chanez, P., Urbach, V., Vachier, I., Godard, P., and Bonnans, C. (2009) Thiazolidinediones induce proliferation of human bronchial epithelial cells through the GPR40 receptor. *Am. J. Physiol. Lung Cell. Mol. Physiol.* **296,** L970–L978
33. Mieczkowska, A., Baslé, M. F., Chappard, D., and Mabilleau, G. (2012) Thiazolidinediones induce osteocyte apoptosis by a G protein-coupled receptor 40-dependent mechanism. *J. Biol. Chem.* **287,** 23517–23526
34. Stoddart, L. A., Brown, A. J., and Milligan, G. (2007) Uncovering the pharmacology of the G protein-coupled receptor GPR40: high apparent constitutive activity in guanosine 5′-*O*-(3-[^{35}S]thio)triphosphate binding studies reflects binding of an endogenous agonist. *Mol. Pharmacol.* **71,** 994–1005
35. Itoh, Y., Kawamata, Y., Harada, M., Kobayashi, M., Fujii, R., Fukusumi, S., Ogi, K., Hosoya, M., Tanaka, Y., Uejima, H., Tanaka, H., Maruyama, M., Satoh, R., Okubo, S., Kizawa, H., Komatsu, H., Matsumura, F., Noguchi, Y., Shinohara, T., Hinuma, S., Fujisawa, Y., and Fujino, M. (2003) Free fatty acids regulate insulin secretion from pancreatic beta cells through GPR40. *Nature* **422,** 173–176
36. Alquier, T., Peyot, M. L., Latour, M. G., Kebede, M., Sorensen, C. M., Gesta, S., Ronald Kahn, C., Smith, R. D., Jetton, T. L., Metz, T. O., Prentki, M., and Poitout, V. (2009) Deletion of GPR40 impairs glucose-induced insulin secretion *in vivo* in mice without affecting intracellular fuel metabolism in islets. *Diabetes* **58,** 2607–2615
37. Kim, H. S., Noh, J. H., Hong, S. H., Hwang, Y. C., Yang, T. Y., Lee, M. S., Kim, K. W., and Lee, M. K. (2008) Rosiglitazone stimulates the release and synthesis of insulin by enhancing GLUT-2, glucokinase and BETA2/NeuroD expression. *Biochem. Biophys. Res. Commun.* **367,** 623–629
38. Yang, C., Chang, T. J., Chang, J. C., Liu, M. W., Tai, T. Y., Hsu, W. H., and Chuang, L. M. (2001) Rosiglitazone (BRL 49653) enhances insulin secretory response via phosphatidylinositol 3-kinase pathway. *Diabetes* **50,** 2598–2602
39. Ptasinska, A., Wang, S., Zhang, J., Wesley, R. A., and Danner, R. L. (2007) Nitric oxide activation of peroxisome proliferator-activated receptor γ through a p38 MAPK signaling pathway. *FASEB J.* **21,** 950–961
40. Hata, K., Nishimura, R., Ikeda, F., Yamashita, K., Matsubara, T., Nokubi, T., and Yoneda, T. (2003) Differential roles of Smad1 and p38 kinase in regulation of peroxisome proliferator-activating receptor γ during bone morphogenetic protein 2-induced adipogenesis. *Mol. Biol. Cell* **14,** 545–555
41. Kliewer, S. A., Umesono, K., Noonan, D. J., Heyman, R. A., and Evans, R. M. (1992) Convergence of 9-*cis* retinoic acid and peroxisome proliferator signalling pathways through heterodimer formation of their receptors. *Nature* **358,** 771–774
42. Yeo, S. J., Gravis, D., Yoon, J. G., and Yi, A. K. (2003) Myeloid differentiation factor 88-dependent transcriptional regulation of cyclooxygenase-2 expression by CpG DNA: role of NF-κB and p38. *J. Biol. Chem.* **278,** 22563–22573
43. Yu, B., Gu, L., and Simon, M. I. (2000) Inhibition of subsets of G protein-coupled receptors by empty mutants of G protein α subunits in G_o, G_{11}, and G_{16}. *J. Biol. Chem.* **275,** 71–76
44. Ge, K., Cho, Y. W., Guo, H., Hong, T. B., Guermah, M., Ito, M., Yu, H., Kalkum, M., and Roeder, R. G. (2008) Alternative mechanisms by which mediator subunit MED1/TRAP220 regulates peroxisome proliferator-activated receptor γ-stimulated adipogenesis and target gene expression. *Mol. Cell. Biol.* **28,** 1081–1091
45. Chu, K. M., Hu, O. Y., Pao, L. H., and Hsiong, C. H. (2007) Pharmacokinetics of oral rosiglitazone in Taiwanese and post hoc comparisons with Caucasian, Japanese, Korean, and mainland Chinese subjects. *J. Pharm. Pharm. Sci.* **10,** 411–419
46. Camp, H. S., Li, O., Wise, S. C., Hong, Y. H., Frankowski, C. L., Shen, X., Vanbogelen, R., and Leff, T. (2000) Differential activation of peroxisome proliferator-activated receptor-γ by troglitazone and rosiglitazone. *Diabetes* **49,** 539–547
47. Maciag, A. E., Holland, R. J., Robert Cheng, Y. S., Rodriguez, L. G., Saavedra, J. E., Anderson, L. M., and Keefer, L. K. (2013) Nitric oxide-releasing prodrug triggers cancer cell death through deregulation of cellular redox balance. *Redox. Biol.* **1,** 115–124
48. Akimoto, T., Pohnert, S. C., Li, P., Zhang, M., Gumbs, C., Rosenberg, P. B., Williams, R. S., and Yan, Z. (2005) Exercise stimulates Pgc-1α transcription in skeletal muscle through activation of the p38 MAPK pathway. *J. Biol. Chem.* **280,** 19587–19593
49. Bordicchia, M., Liu, D., Amri, E. Z., Ailhaud, G., Dessì-Fulgheri, P., Zhang, C., Takahashi, N., Sarzani, R., and Collins, S. (2012) Cardiac natriuretic peptides act via p38 MAPK to induce the brown fat thermogenic program in mouse and human adipocytes. *J. Clin. Invest.* **122,** 1022–1036
50. Puigserver, P., Adelmant, G., Wu, Z., Fan, M., Xu, J., O'Malley, B., and Spiegelman, B. M. (1999) Activation of PPARγ coactivator-1 through transcription factor docking. *Science* **286,** 1368–1371
51. Gelman, L., Zhou, G., Fajas, L., Raspé, E., Fruchart, J. C., and Auwerx, J. (1999) p300 interacts with the N- and C-terminal part of PPARγ2 in a ligand-independent and -dependent manner, respectively. *J. Biol. Chem.* **274,** 7681–7688
52. Wang, Q. E., Han, C., Zhao, R., Wani, G., Zhu, Q., Gong, L., Battu, A., Racoma, I., Sharma, N., and Wani, A. A. (2013) p38 MAPK- and Akt-mediated p300 phosphorylation regulates its degradation to facilitate nucleotide excision repair. *Nucleic Acids Res.* **41,** 1722–1733
53. Handschin, C., and Spiegelman, B. M. (2006) Peroxisome proliferator-activated receptor γ coactivator 1 coactivators, energy homeostasis, and metabolism. *Endocr. Rev.* **27,** 728–735
54. Maekawa, T., Jin, W., and Ishii, S. (2010) The role of ATF-2 family transcription factors in adipocyte differentiation: antiobesity effects of p38 inhibitors. *Mol. Cell. Biol.* **30,** 613–625
55. Lennon, A. M., Ramaugé, M., Dessouroux, A., and Pierre, M. (2002) MAP kinase cascades are activated in astrocytes and preadipocytes by 15-deoxy-Δ(12–14)-prostaglandin J(2) and the thiazolidinedione ciglitazone through peroxisome proliferator activator receptor γ-independent mechanisms involving reactive oxygenated species. *J. Biol. Chem.* **277,** 29681–29685
56. Duan, S. Z., Ivashchenko, C. Y., Russell, M. W., Milstone, D. S., and Mortensen, R. M. (2005) Cardiomyocyte-specific knockout and agonist of peroxisome proliferator-activated receptor-γ both induce cardiac hypertrophy in mice. *Circ. Res.* **97,** 372–379

57. Gardner, O. S., Shiau, C. W., Chen, C. S., and Graves, L. M. (2005) Peroxisome proliferator-activated receptor γ-independent activation of p38 MAPK by thiazolidinediones involves calcium/calmodulin-dependent protein kinase II and protein kinase R: correlation with endoplasmic reticulum stress. *J. Biol. Chem.* **280,** 10109–10118
58. Sugawara, Y., Nishii, H., Takahashi, T., Yamauchi, J., Mizuno, N., Tago, K., and Itoh, H. (2007) The lipid raft proteins flotillins/reggies interact with $G\alpha_q$ and are involved in G_q-mediated p38 mitogen-activated protein kinase activation through tyrosine kinase. *Cell. Signal.* **19,** 1301–1308
59. Wallberg, A. E., Yamamura, S., Malik, S., Spiegelman, B. M., and Roeder, R. G. (2003) Coordination of p300-mediated chromatin remodeling and TRAP/mediator function through coactivator PGC-1α. *Mol. Cell* **12,** 1137–1149
60. Rodgers, J. T., and Puigserver, P. (2007) Fasting-dependent glucose and lipid metabolic response through hepatic sirtuin 1. *Proc. Natl. Acad. Sci. U.S.A.* **104,** 12861–12866
61. Gerhart-Hines, Z., Rodgers, J. T., Bare, O., Lerin, C., Kim, S. H., Mostoslavsky, R., Alt, F. W., Wu, Z., and Puigserver, P. (2007) Metabolic control of muscle mitochondrial function and fatty acid oxidation through SIRT1/PGC-1α. *EMBO J.* **26,** 1913–1923
62. Nasrin, N., Kaushik, V. K., Fortier, E., Wall, D., Pearson, K. J., de Cabo, R., and Bordone, L. (2009) JNK1 phosphorylates SIRT1 and promotes its enzymatic activity. *PloS One* **4,** e8414
63. Wang, L., Zhang, L., Chen, Z. B., Wu, J. Y., Zhang, X., and Xu, Y. (2009) Icariin enhances neuronal survival after oxygen and glucose deprivation by increasing SIRT1. *Eur. J. Pharmacol.* **609,** 40–44
64. Hong, E. H., Lee, S. J., Kim, J. S., Lee, K. H., Um, H. D., Kim, J. H., Kim, S. J., Kim, J. I., and Hwang, S. G. (2010) Ionizing radiation induces cellular senescence of articular chondrocytes via negative regulation of SIRT1 by p38 kinase. *J. Biol. Chem.* **285,** 1283–1295
65. Fernandez-Pisonero, I., Duenas, A. I., Barreiro, O., Montero, O., Sanchez-Madrid, F., and Garcia-Rodriguez, C. (2012) Lipopolysaccharide and sphingosine-1-phosphate cooperate to induce inflammatory molecules and leukocyte adhesion in endothelial cells. *J. Immunol.* **189,** 5402–5410
66. Tanaka, H., Yoshida, S., Oshima, H., Minoura, H., Negoro, K., Yamazaki, T., Sakuda, S., Iwasaki, F., Matsui, T., and Shibasaki, M. (2013) Chronic treatment with novel GPR40 agonists improve whole-body glucose metabolism based on the glucose-dependent insulin secretion. *J. Pharmacol. Exp. Ther.* **346,** 443–452
67. Rajagopal, S., Rajagopal, K., and Lefkowitz, R. J. (2010) Teaching old receptors new tricks: biasing seven-transmembrane receptors. *Nat. Rev. Drug Discov.* **9,** 373–386
68. DeWire, S. M., and Violin, J. D. (2011) Biased ligands for better cardiovascular drugs: dissecting G-protein-coupled receptor pharmacology. *Circ. Res.* **109,** 205–216